Surg Today (2013) 43:289–292
DOI 10.1007/s00595-012-0462-8

ORIGINAL ARTICLE

A rare point mutation in the Ras oncogene in hepatocellular carcinoma

Akinobu Taketomi · Ken Shirabe · Jun Muto · Shohei Yoshiya · Takashi Motomura · Yohei Mano · Tohru Ikegami · Tomoharu Yoshizumi · Kenji Sugio · Yoshihiko Maehara

Received: 16 May 2011 / Accepted: 17 May 2011 / Published online: 26 December 2012

Abstract
Purpose The Ras gene is one of the oncogenes most frequently detected in human cancers, and codes for three proteins (K-, N-, and H-Ras). The aim of this study was to examine the mutations in codons 12, 13 and 61 of the three Ras genes in cases of human hepatocellular carcinoma (HCC).
Methods Paired samples of HCC and corresponding non-malignant liver tissue were collected from 61 patients who underwent hepatectomy. A dot-blot analysis was used to analyze the products of the polymerase chain reaction (PCR) amplification of codons 12, 13, and 61 of K-, N- and H-Ras for mutations.
Results Only one mutation (K-Ras codon 13; Gly to Asp) was detected among the 61 patients. Interestingly, this patient had a medical history of surgery for both gastric cancer and right lung cancer. No mutations were found in codons 12 and 61 of K-Ras or codons 12, 13 and 61 of the N-Ras and H-Ras genes in any of the HCCs or corresponding non-malignant tissues.
Conclusions These findings indicated that the activation of Ras proto-oncogenes by mutations in codons 12, 13, and 61 does not play a major role in hepatocellular carcinogenesis.

Keywords Ras · Mutation · Hepatocellular carcinoma · Sorafenib

A. Taketomi (✉) · K. Shirabe · J. Muto · S. Yoshiya · T. Motomura · Y. Mano · T. Ikegami · T. Yoshizumi · K. Sugio · Y. Maehara
Department of Surgery and Science, Graduate School of Medical Sciences, Kyushu University, 3-1-1 Maidashi, Higashi-ku, Fukuoka, Japan
e-mail: taketomi@med.hokudai.ac.jp; taketomi@surg2.med.kyushu-u.ac.jp

Abbreviations

Asp	Asparagine
Glu	Glutamate
Gly	Glycine
HCC	Hepatocellular carcinoma
Lys	Lysine
PCR	Polymerase chain reaction
TTP	Time to progression
Val	Valine

Introduction

Hepatocellular carcinoma (HCC) is a global health problem, accounting for more than 80 % of all primary liver cancers, and is one of the most common malignancies worldwide [1]. Most patients with HCC also present with concomitant cirrhosis, which is the major clinical risk factor for hepatic cancer, and results from alcoholism or infection with the hepatitis B or hepatitis C virus. Primary liver malignancies (95 % of which are HCC) are the third and fifth leading causes of cancer death among males and females, respectively, in Japan [2]. Both liver resection and liver transplantation are potentially curative treatments for HCC [3–5]. Although other treatment options, including percutaneous radiofrequency ablation or chemolipiodolization are also available, there is no standard systemic therapy for advanced cases.

Sorafenib (BAY 43-9006, Nexavar) is a novel oral kinase inhibitor that targets multiple tyrosine kinases in vivo and in vitro, and is widely used for HCC [6]. The main targets of sorafenib are the receptor tyrosine kinase pathways which are frequently deregulated in cancer, such as the Ras pathway. The Ras pathway represents a dominant signaling network promoting cell proliferation and

survival. The binding of different growth factors (e.g. epidermal growth factor: EGF) to their receptors (e.g. epidermal growth factor receptor: EGFR) induces the activation of Ras, which in turn activates c-raf, MEK and ERK. Phosphorylated ERK in the nucleus activates transcription factors that regulate the expression of genes involved in cell proliferation and survival.

A phase II trial involving 137 patients with advanced HCC showed that sorafenib induced partial responses in less than 5 % of patients, but the observed median survival of 9.2 months with a median time to progression of 5.5 months was classified as evidence of potential clinical benefit, since the expected median survival of these patients is 6 months [7]. Consequently, a large phase III clinical trial (SHARP) was conducted in 602 patients with advanced HCC. The results showed a 31 % decrease in the risk of death, with a median survival of 10.6 months in the sorafenib arm versus 7.9 months for placebo [8]. In addition, sorafenib showed a significant benefit in terms of the time to progression (TTP) as assessed by independent radiological review, with a median TTP of 5.5 months for the sorafenib and 2.8 months for the placebo arm.

Because Ras is one of the targets of sorafenib, it is important to determine whether mutations in the Ras gene result in the activation of the Ras/MAPK pathway in human HCCs. However, the relationship between Ras mutations and human HCC has not been fully evaluated. The present study was designed to investigate K-, N- and H-Ras (*KRAS, NRAS, HRAS*) somatic mutations in human HCC.

Materials and methods

Patients and tumor samples

Tumor tissue samples were obtained from 61 Japanese patients who underwent surgical resection for HCC during the period between December 1989 and April 1992 in the Department of Surgery and Science, Kyushu University Hospital, Fukuoka, Japan. Surgically resected tissue samples were frozen at −80 °C immediately after resection and were stored until use in this study. Written informed consent was obtained from all patients examined, and the current study was approved by the Kyushu University ethics committee.

DNA preparation and detection of Ras point mutations

High molecular weight DNA was isolated from frozen tumor samples, as described elsewhere [9]. Selective amplification of the Ras gene sequence was done using a PCR technique. The nucleotide sequences of the primers used are listed in Table 1. The PCR was performed at

Table 1 Ras gene primers used in this study

Gene/codon	Length (bp)	Sequence	
KRAS/12, 13	108	Forward	GACTGAATATAAACTTGTGG
		Reverse	CTATTGTTGGATCATATTCG
KRAS/61	128	Forward	TTCCTACAGGAAGCAAGTAG
		Reverse	CACAAAGAAAGCCCTCCCCA
HRAS/12, 13	63	Forward	GACGGAATATAAGCTGGTGG
		Reverse	TGGATGGTCAGCGCACTCTT
HRAS/61	73	Forward	AGACGTGCCTGTTGGACATC
		Reverse	CGCATGTACTGGTCCCGCAT
NRAS/12, 13	109	Forward	GACTGAGTACAAACTGGTGG
		Reverse	CTCTATGGTGGGATCATATT
NRAS/61	103	Forward	GGTGAAACCTGTTTGTTGGA
		Reverse	ATACACAGAGGAAGCCTTCG

bp base pairs

96 °C to denature the DNA (1 min), at 55 °C (*NRAS*), 57 °C (*KRAS*), 62 °C (*HRAS*) to anneal the primer (30 s), and at 72 °C to synthesize DNA (10 s to 1 min) using Taq DNA polymerase for 35–40 cycles in a DNA thermal cycler (Perkin-Elmer-Cetus). Amplified DNA samples were spotted onto nylon membranes (Hybond N+) for the hybridization analysis. All of the DNA isolated from the 61 tumor samples and the corresponding non-malignant liver tissues were screened for activated point mutations in codons 12, 13, and 61 of all three Ras genes using an oligonucleotide specific for the different sequences. The filters were prehybridized for 1 h at 55 °C in solution A (3.0 M tetramethylammonium chloride, 50 mM Tris-HCI, 2 HIMEDTA, 0.1 % SDS, 5× Denhardt's solution, 100 fg/ml denatured herring sperm DNA), and hybridized for 1 h at 55 °C in the same solution with 5 pmol ^{32}P-labeled probe. These filters were washed twice in 0.3 M NaCl, 0.02 M NaH2PO4, 2 mM EDTA and 0.1 % SDS at room temperature for 5 min, and in solution A without Denhardt's solution and herring sperm DNA, once for 5 min at room temperature and twice for 10 min at 60 °C. These filters were then exposed to Kodak XAR5 film. Human cancer cell lines carrying Ras genes mutations were used as positive controls. The colon cancer cell lines: SW620 (*KRAS* codon 12 GTT:Val), LSI80 (*KRAS* codon 12 GAT:Asp), and LOVO (*KRAS* codon 13 GAC:Asp) were obtained from the Japanese Cancer Research Resources Bank, and KMS4 (*KRAS*s codon 12 TGT:Cys) was provided by Dr. Sugio (Institution?).

Results

The age of the 61 patients ranged from 43 to 79 years (average, 64.1 years), and 46 were males and 15 were

females. The positive rate of hepatitis surface B antigen was 12.9 %, and the positive rate of anti-hepatitis C virus antibody was 72.7 %. The mean tumor size was 4.47 cm.

One of the 61 HCCs (1.6 %) carried a point mutation, which was a G to A transition at codon 13 of the *KRAS* gene (Fig. 1). DNA extracted from the corresponding non-malignant liver tissue had the normal codon, suggesting that mutational activation of K-ras was involved in the malignant transformation in this case. This patient was positive for anti-hepatitis C virus antibodies, and was classified to have Child-Pugh A disease. The diameter of this patient's tumor was 12 cm, and the tumor was composed of well to moderately differentiated hepatocellular carcinoma. Interestingly, this patient had undergone surgery for gastric cancer 18 years before and lung cancer 12 years before the surgery for HCC.

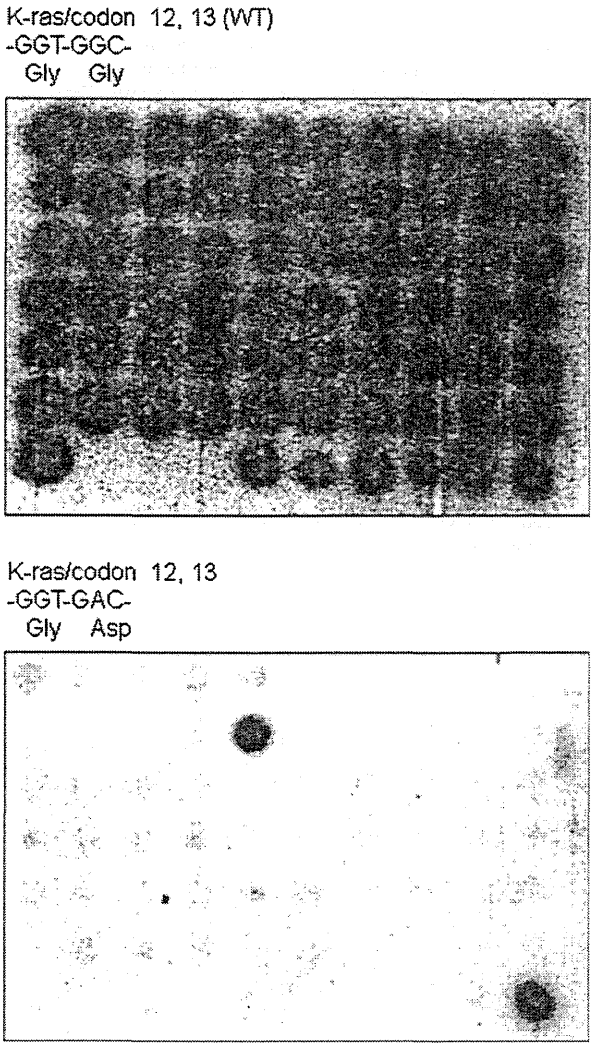

Fig. 1 Detection of a *KRAS* gene mutation in a patient with hepatocellular carcinoma. PCR-amplified DNA from 61 tumor samples was dotted onto nylon membranes and hybridized to a ^{32}P-labeled oligonucleotide probe. *WT* wild type *KRAS*

No mutational activation was found in codons 12 and 61 of *KRAS* or codons 12, 13 and 61 of the *NRAS* and *HRAS* genes in any of the HCCs or corresponding non-malignant tissue samples.

Discussion

This study examined 61 HCC tissues and their corresponding non-malignant liver tissues for a somatic mutation in codons 12, 13, and 61 of the *KRAS*, *HRAS*, or *NRAS* genes, which are known hot spots in various malignancies. However, the study showed the only one of the 61 HCCs (1.6 %) had a somatic mutation in codon 13 of the *KRAS* gene, indicating that Ras gene mutations do not appear to be related to the pathogenesis of most HCCs.

There have been several reports with small sample sizes regarding Ras gene mutations in HCC (Table 2). Most have reported that somatic mutations of the Ras gene in HCCs are uncommon, similar to the current study. Tsuda et al. [10] found only two tumors with Ras point mutations in surgically resected specimens from 30 HCC patients. In their patients, codon 12 of *KRAS* was altered from GGT, coding for Gly, to GTT, coding for Val in one case, and codon 61 of *NRAS* was altered from CAA, coding for Glu, to AAA, coding for Lys, in the other case. Tada et al. analyzed the mutations of the three Ras genes in 23 primary hepatic malignant tumors (12 hepatocellular carcinomas, nine cholangiocarcinomas, and two hepatoblastomas). Point mutations in *KRAS* codon 12 or *KRAS* codon 61 were found in 6 of the 9 cholangiocarcinomas. In contrast, there were no point mutations in any of 12 HCCs or two hepatoblastomas in codons 12, 13, or 61 of the Ras genes. The authors concluded that Ras gene mutations are not related to the pathogenesis of HCC, but play an important role in pathogenesis of cholangiocarcinoma.

Sorafenib is the first molecule with specific targets involved in the pathogenesis of HCC that has become available for routine clinical use. It is an orally applicable

Table 2 Reported Ras gene mutations in HCC patients

Author [references]	No. of patients	Ras gene mutation		
		KRAS	*NRAS*	*HRAS*
Tsuda et al. [10]	30	1 (codon 12)	1 (codon 61)	0
Tada et al. [14]	12	0	0	0
Ogata et al. [15]	19			2
Challen et al. [16]	19	1 (codon 61)	3 (codon 61)	0
Leon et al. [17]	12	1 (codon 61)	0	0
This study	61	1 (codon 13)	0	0

multi-kinase inhibitor that acts by blocking tumor cell proliferation and angiogenesis through the inhibition of serine/threonine kinases [11]. Sorafenib can increase survival by up to 3 months in patients with advanced HCC and acceptable liver function [8]. On the other hand, severe side effects have been reported with sorafenib, including hand-foot skin reactions or liver dysfunction [7, 8]. Therefore, it is important to identify prognostic markers and to establish the proper selection criteria for using sorafenib. Mutations of the Ras genes in cases of HCCs were systemically evaluated in this study because the Ras signaling pathway is the main target of sorafenib. The results indicated that mutational activation of Ras genes is uncommon in the pathogenesis of HCCs. Caraglia et al. [12] reported that the presence of phosphorylated ERK activity in peripheral blood mononuclear cells is valuable for predicting the response to sorafenib therapy in HCC patients. An in vitro study confirmed that phosphorylated ERK was a potential biomarker predicting the sensitivity of HCC to sorafenib [13]. Therefore, a mutation in the RAF/MEK/ERK pathway may be involved in the drug resistance to sorafenib, rather than a Ras mutation.

In summary, only one of 61 HCCs (1.6 %) in the present study carried a point mutation, which was a G to A transition in codon 13 of the *KRAS* gene. No mutational activation was found in codons 12 and 61 of *KRAS* or in codons 12, 13 and 61 of the *NRAS* or *HRAS* genes in any of the HCCs or corresponding non-malignant tissue samples. These findings suggested that Ras gene mutations are not related to the pathogenesis of most HCCs. The signaling pathways downstream of Ras should be examined to identify markers to predict a response to sorafenib.

Acknowledgments We thank Professor Brian Quinn for his review of this manuscript. No financial support was received for this work from any company. This study was supported in part by a grant from the Scientific Research Fund of the Ministry of Education of Japan.

Conflict of interest None of the authors has any conflict of interest.

References

1. El Serag HB, Rudolph KL. Hepatocellular carcinoma: epidemiology and molecular carcinogenesis. Gastroenterology. 2007;132:2557–76.
2. Okita K. Clinical aspects of hepatocellular carcinoma in Japan. Intern Med. 2006;45:229–33.
3. Taketomi A, Kitagawa D, Itoh S, Harimoto N, Yamashita Y, Gion T, et al. Trends in morbidity and mortality after hepatic resection for hepatocellular carcinoma: an institute's experience with 625 patients. J Am Coll Surg. 2007;204:580–7.
4. Taketomi A, Sanefuji K, Soejima Y, Yoshizumi T, Uhciyama H, Ikegami T, et al. Impact of des-gamma-carboxy prothrombin and tumor size on the recurrence of hepatocellular carcinoma after living donor liver transplantation. Transplantation. 2009;87:531–7.
5. Llovet JM, Schwartz M, Mazzaferro V. Resection and liver transplantation for hepatocellular carcinoma. Semin Liver Dis. 2005;25:181–200.
6. Llovet JM, Bruix J. Molecular targeted therapies in hepatocellular carcinoma. Hepatology. 2008;48:1312–27.
7. Abou Alfa GK, Schwartz L, Ricci S, Amadori D, Santoro A, Figer A, et al. Phase II study of sorafenib in patients with advanced hepatocellular carcinoma. J Clin Oncol. 2006;24:4293–300.
8. Llovet JM, Ricci S, Mazzaferro V, Hilgard P, Gane E, Blanc JF, et al. Sorafenib in advanced hepatocellular carcinoma. N Engl J Med. 2008;359:378–90.
9. Sugio K, Ishida T, Yokoyama H, Inoue T, Sugimachi K, Sasazuki T. Ras gene mutations as a prognostic marker in adenocarcinoma of the human lung without lymph node metastasis. Cancer Res. 1992;52:2903–6.
10. Tsuda H, Hirohashi S, Shimosato Y, Ino Y, Yoshida T, Terada M. Low incidence of point mutation of c-Ki-ras and N-ras oncogenes in human hepatocellular carcinoma. Jpn J Cancer Res. 1989;80:196–9.
11. Tanaka S, Arii S. Current status of molecularly targeted therapy for hepatocellular carcinoma: basic science. Int J Clin Oncol. 2010;15:235–41.
12. Caraglia M, Giuberti G, Marra M, Addeo R, Montella L, Murolo M, et al. Oxidative stress and ERK1/2 phosphorylation as predictors of outcome in hepatocellular carcinoma patients treated with sorafenib plus octreotide LAR. Cell Death Dis. 2011;2:e150.
13. Zhang Z, Zhou X, Shen H, Wang D, Wang Y. Phosphorylated ERK is a potential predictor of sensitivity to sorafenib when treating hepatocellular carcinoma: evidence from an in vitro study. BMC Med. 2009;7:41.
14. Tada M, Omata M, Ohto M. Analysis of ras gene mutations in human hepatic malignant tumors by polymerase chain reaction and direct sequencing. Cancer Res. 1990;50:1121–4.
15. Ogata N, Kamimura T, Asakura H. Point mutation, allelic loss and increased methylation of c-Ha-ras gene in human hepatocellular carcinoma. Hepatology. 1991;13:31–7.
16. Challen C, Guo K, Collier JD, Cavanagh D, Bassendine MF. Infrequent point mutations in codons 12 and 61 of ras oncogenes in human hepatocellular carcinomas. J Hepatol. 1992;14:342–6.
17. Leon M, Kew MC. Analysis of ras gene mutations in hepatocellular carcinoma in southern African blacks. Anticancer Res. 1995;15:859–61.

Original Paper

Pathobiology

Pathobiology 2013;80:146–154
DOI: 10.1159/000346196

Received: August 29, 2012
Accepted after revision: November 27, 2012
Published online: January 25, 2013

Tumor-Associated Macrophage Promotes Tumor Progression via STAT3 Signaling in Hepatocellular Carcinoma

Yohei Mano[a, b] Shinichi Aishima[a] Nobuhiro Fujita[c] Yuki Tanaka[a]
Yuichiro Kubo[a] Takashi Motomura[b] Akinobu Taketomi[b] Ken Shirabe[b]
Yoshihiko Maehara[b] Yoshinao Oda[a]

Departments of [a]Anatomic Pathology, [b]Surgery and Science, and [c]Clinical Radiology, Graduate School of Medical Sciences, Kyushu University, Fukuoka, Japan

Key Words
Hepatocellular carcinoma · STAT3 · Macrophage

Abstract
Objective: Signal transducer and activator of transcription 3 (STAT3) is activated in hepatocellular carcinoma (HCC), and tumor-associated macrophage plays an important role in tumor progression. Therefore, we examined STAT3 activation, cytokine expression and infiltration of tumor-associated macrophages in resected HCCs as well as the alteration of cell growth and migration by cytokine stimulation in HCC cell lines. ***Methods:*** Immunohistochemical staining of phosphorylated STAT3 (pSTAT3), CD163, interleukin (IL)-6, Ki-67 and Bcl-XL was performed for 101 cases of resected HCC, and correlations between pSTAT3 staining and clinicopathological findings were analyzed. In HCC cell lines (PLC/PRF/5 and Huh7), cell proliferation and migration by IL-6 stimulation and S3I-201 (STAT3 inhibitor) treatment were analyzed. ***Results:*** In HCC specimens, the pSTAT3-positive group showed high levels of α-fetoprotein ($p = 0.0276$), large tumor size ($p = 0.0092$), frequent intrahepatic metastasis ($p = 0.0214$), high Ki-67 ($p = 0.0002$) and Bcl-XL ($p = 0.0001$), poor prognosis ($p = 0.0234$), and high recurrence rate ($p = 0.0003$). CD163-positive cells were frequently observed in the pSTAT3-positive group ($p = 0.0013$). In two HCC cell lines, IL-6 stimulation promoted cell proliferation and migration via the STAT3 phosphorylation, and S3I-201 inhibited this activation. ***Conclusions:*** STAT3 activation was correlated with aggressive behavior of HCC and may be mediated via tumor-associated macrophage. We expect that STAT3 signaling and tumor-associated macrophages can be attractive therapeutic targets in HCC patients.

Introduction

Hepatocellular carcinoma (HCC) is the fifth most common cause of cancer in the world [1]. Although surgical therapies for HCC have progressed and outcomes of HCC have improved, HCC still often recurs after surgery [2, 3]. Sorafenib, one of the molecular targeted therapies, was reported to show activity against unresectable HCCs;

KARGER

Fax +41 61 306 12 34
E-Mail karger@karger.ch
www.karger.com

1015–2008/13/0803–0146$38.00/0

Accessible online at:
www.karger.com/pat

Yoshinao Oda, PhD
Department of Anatomic Pathology
Graduate School of Medical Sciences, Kyushu University
3-1-1 Maidashi, Higashi-ku, Fukuoka 812-8582 (Japan)
E-Mail oda@surgpath.med.kyushu-u.ac.jp

however, its survival advantage is only 3.7 months [4]. New therapeutic targets are required to improve the survival of patients with HCC.

Signal transducer and activator of transcription 3 (STAT3) is an important molecule in tumor progression [5]. STAT3 activation occurs via phosphorylation and dimerization of tyrosine residue (Tyr705), leading to nuclear entry, DNA binding and gene transcription. STAT3 was regarded as a critical transcription activator for cell cycle- or cell survival-related genes. Bcl-XL is an antiapoptotic protein transcribed by STAT3 activation [6]. Some cytokines such as interleukin (IL)-6 or IL-10 activate STAT3 signaling via their receptors [7]. Constitutive activation of STAT3 has been demonstrated to contribute to tumorigenesis in breast cancer [8], colon cancer [9], lung cancer [10], pancreatic cancer [11], prostate cancer [12], and melanoma [13]. In human HCC, STAT3 phosphorylation was also detected and related to tumor progression [14], angiogenesis [15] and tumorigenesis [16]. The tumor microenvironment is closely associated with the growth of tumor cells, and tumor-associated macrophages play an important role in tumor progression [17]. Macrophages are major inflammatory cells that infiltrate tumors; several studies have shown that high infiltration of tumor-associated macrophages was associated with tumor progression and metastasis [17–20] and predicts poor prognosis in patients with HCC [21]. Tumor-associated macrophages activate STAT3 in ovarian cancer [22] and glioblastoma [23]. However, the correlation between tumor-associated macrophages and STAT3 activation of HCC tumor cells is unknown. Therefore, we examined STAT3 activation, cytokine expression and infiltration of tumor-associated macrophages in resected HCCs and analyzed their association with clinicopathological findings. Alterations in cell growth and migration by cytokine stimulation and STAT3 inhibitor were also analyzed in HCC cell lines.

Materials and Methods

Patients and Samples

One hundred and one available paraffin-embedded specimens from patients with HCC who underwent hepatectomy between January 1997 and December 2001 in our institute were selected by reviewing their pathology data. Any patients undergoing previous or noncurative surgery were excluded. After the surgery, monthly measurement of the serum α-fetoprotein (AFP) level was performed. In addition, ultrasonography and dynamic CT were performed every 3 months. The postoperative survival period or recurrence was entered into the database immediately when a patient died or if recurrence was strongly suspected on diagnostic imaging such as CT or magnetic resonance imaging.

This study conformed to the ethical guidelines of the 1975 Declaration of Helsinki and was approved by the ethics committees of Kyushu University Hospital (grant No. 21-117). Informed consent was obtained from each patient included in the study.

Immunohistochemistry

Sections of resected specimens were fixed in 10% buffered formalin, embedded in paraffin and stained by Envision+ system and DAB kit (Dako, Glostrup, Denmark). Immunohistochemical stains were performed with antibodies of phosphorylated STAT3 (pSTAT3; Tyr 705; D3A7, 1:50; Cell Signaling Technology), CD163 (10D6, 1:200; Novocastra), IL-6 (rabbit polyclonal, 1:1,000; Abcam), Ki-67 (MIB-1, 1:200; Dako), and Bcl-XL (rabbit polyclonal, 1:200; Santa Cruz Biotechnology, Santa Cruz, Calif., US). Sections were pretreated before being incubated with primary antibodies in a microwave oven at 99°C for 20 min for pSTAT3, CD163, IL-6 and Bcl-XL or in a pressure cooker for 25 min for Ki-67.

Each slide was stained in serial sections and examined by two pathologists (Y.M. and S.A.). In nuclear staining of pSTAT3 and Ki-67 and in cytoplasm staining of Bcl-XL, the percent positive cells was estimated by count of 1,000 tumor cells in most staining areas (hot spots). Staining of CD163, a marker of tumor-associated macrophages [19, 22–25], and IL-6 was evaluated by estimating the total counts of cytoplasm or membrane at 3 high-power fields. The mean of nuclear pSTAT3-positive cells in HCCs was 10.7% (range 0–82.0), and pSTAT3 stain was classified into a positive (≥10.7% of tumor cell nuclei) and a negative group (<10.7% of tumor nuclei). Furthermore, in the cases of the pSTAT3-positive group (n = 36), the CD163-positive cells were counted separately in areas of pSTAT3-positive and pSTAT3-negative HCC cells.

For double staining of IL-6 and CD163, HCC specimens were boiled in 10 mM citrate buffer (pH 6.0) for 20 min and incubated with IL-6 primary antibody (1:1,000) at room temperature for 15 min. The sections were washed three times and incubated with anti-rabbit horseradish peroxidase-conjugated polymer at room temperature for 45 min; IL-6 was visualized by DAB kit. Next, the sections were boiled in 10 mM citrate buffer (pH 6.0) for 10 min, incubated with CD163 primary antibody (1:200) for 90 min and incubated with anti-mouse alkaline phosphatase-conjugated polymer at room temperature for 45 min. CD163 of the sections was visualized by New Fuchsin Substrate kit (Nichirei, Tokyo, Japan).

Cell Culture

Human HCC cell lines PLC/PRF/5 and Huh7 were obtained from Riken Bioresource Center, Tsukuba, Japan, and cultured in Dulbecco's modified Eagle's medium (DMEM) supplemented with 1 or 10% fetal bovine serum (FBS). PLC/PRF/5 and Huh7 cells were maintained in DMEM containing 1% FBS for 24 h prior to IL-6 (Peprotech, Rocky Hill, N.J., USA) stimulation. All in vitro experiments were done in triplicate.

Immunoblotting

Cellular proteins were solubilized in lysis buffer containing protease inhibitor and phosphatase inhibitor 30 min after stimulation with IL-6 (20 μg/ml). Equal amounts of protein were separated by SDS-PAGE and then transferred to the polyvinylidene fluoride membrane. Following blocking in Tris buffer containing 2% BSA, the membrane was stained with 1:1,000 dilution of anti-STAT3 (Cell Signaling Technology, Danvers, Mass., USA) and anti-pSTAT3 (Cell Signaling Technology) antibodies, then

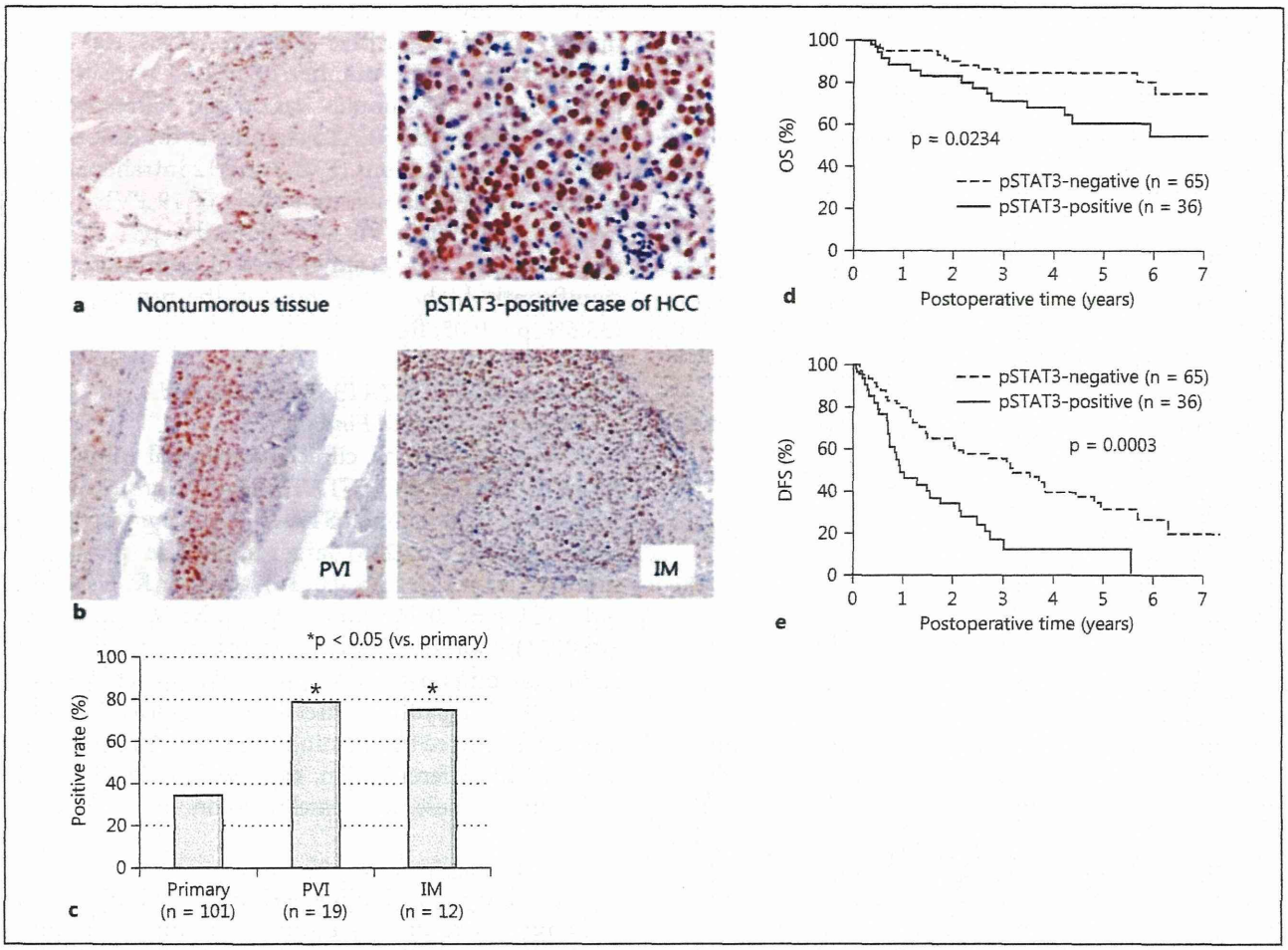

Fig. 1. Immunohistochemical staining of pSTAT3 in HCC. **a** pSTAT3 was expressed in the nucleus. In nontumorous tissue, endothelial cells, bile duct epithelial cells and inflammatory cells were stained by pSTAT3 (left panel). ×100. HCC cells were also stained (82.2%, right panel). ×100. **b** Tumor cells of PVI and IM stained by pSTAT3. ×200. **c** Comparison of pSTAT3 staining in primary HCC, tumor cells of PVI and IM. pSTAT3 staining was significantly prominent in tumor cells of PVI and IM compared with primary HCC ($p < 0.05$). **d**, **e** pSTAT3 expression correlated with poor prognosis. OS (**d**) and DFS (**e**) curves for pSTAT3-positive and pSTAT3-negative groups in patients with HCC (**d**, $p = 0.0234$; **e**, $p = 0.0003$; log-rank test).

washed and incubated with horseradish peroxidase-conjugated secondary antibody (Cell Signaling Technology). Bands were visualized by the enhanced chemiluminescence system (GE Healthcare, UK).

Cell Growth Assay

PLC/PRF/5 and Huh7 cells were seeded at a density of 5×10^4 cells/24-well plates and maintained in conditioned medium for 24 h before stimulation. Viable cells were counted by trypan blue stain 48 h after stimulation with IL-6 (25 ng/ml).

Wound-Healing Assay

PLC/PRF/5 and Huh7 cells were seeded at a density of 5×10^4 cells/6-well plates. Approximately 24 h later, when the cells were 100% confluent, a sterile 100-μl pipette tip was used to longitudinally scratch a constant-diameter strip in the confluent monolayer. The medium and cell debris were aspirated away and replaced by 2 ml of fresh DMEM containing 1% FBS with or without IL-6 (25 ng/ml). Photographs were taken at 0 and 48 h after wounding by phase-contrast microscopy. For statistical analysis, three randomly selected points along each wound were marked, and the horizontal distance between the migrating cells and the initial wound was measured 48 h later.

Inhibition of STAT3

In both cell growth and wound-healing assays, PLC/PRF/5 and Huh7 cells were cultured in DMEM containing 1% FBS and IL-6 (25 ng/ml) with or without 100 nM S3I-201 (NSC 74859; Santa Cruz Biotechnology). S3I-201 was treated 30 min before IL-6 stimulation. DMSO was used for control.

Table 1. Comparison of pSTAT3 expression and clinicopathological findings

pSTAT3 expression	pSTAT3 negative (n = 65)	pSTAT3 positive (n = 36)	p value
Clinical features			
Sex, male/female	55/10	26/10	0.0849
Age, years	63.9±7.3	63.6±9.5	0.8726
HBsAg, +/–	14/51	8/28	0.9922
HCV Ab, +/–	42/23	23/13	0.9798
Cirrhosis	22/43	14/22	0.4990
AFP, ng/ml	852.4±308†	20,673.4±11,688†	0.0276*
DCP, mAU/ml	2,798.2±1,179.1†	6,278.4±3,184.7†	0.2217
Pathological features			
Tumor size, cm	3.7±2.2	5.1±3.2	0.0092*
Differentiation, poor/well and moderate	19/46	16/20	0.1253
Capsule formation	41/24	26/10	0.4619
Infiltration to the capsule	33/32	23/13	0.1681
Portal venous invasion, +/–	30/35	24/12	0.0687
Hepatic venous invasion, +/–	15/50	12/24	0.3031
Intrahepatic metastasis, +/–	18/47	18/18	0.0214*
MIB-1 LI, %	3.5±0.5	10.2±2.2	0.0002*
Bcl-XL, %	13.0±1.5	25.2±2.0	0.0001*

HBsAg = Hepatitis B surface antigen; HCV Ab = hepatitis C virus antibody; DCP = des-γ-carboxy prothorombin. * $p < 0.05$.

Statistical Analysis

Statistical analysis was carried out using Microsoft Excel software and JMP software (SAS Institute, Cary, N.C., USA). Comparison between pSTAT3 staining and clinicopathological findings or staining of other antibodies was evaluated by Pearson's χ^2, Fisher's exact tests and the Mann-Whitney U test. Patient survival analysis including overall survival (OS) and disease-free survival (DFS) was calculated by the Kaplan-Meier method; differences were evaluated by the log-rank test. For multivariate analysis, the Cox proportional hazard model was used. Two-sided Student's t test was applied for analysis of in vitro data. Statistical analyses were considered significant at a p value <0.05.

Results

pSTAT3 Expression in Clinical Samples

pSTAT3 was stained in the nuclei of HCC cells, normal endothelial cells, some bile duct epithelial cells and inflammatory cells. pSTAT3 nuclear staining in HCC cells is displayed in figure 1a. The mean percentage of nuclear pSTAT3-positive cells in HCCs was 10.7% (range 0–82.0). The number of pSTAT3-positive and pSTAT3-negative samples was 36 and 65, respectively. We also examined pSTAT3 staining at the lesions of 19 portal venous invasions (PVIs) and 12 intrahepatic metastases (IMs) in 101 cases. Fifteen of 19 PVIs (78.9%) and 9 of 12 (75.0%) IMs were defined as pSTAT3-positive cases (fig. 1b). Positive rates in both lesions were significantly higher than those in the primary lesions (35.6%; $p < 0.05$; fig. 1c).

Comparison of pSTAT3 Expression and Clinicopathological Findings

A comparison of clinicopathological findings in pSTAT3-positive and pSTAT3-negative groups is summarized in table 1. The pSTAT3-positive group showed higher AFP ($p = 0.0276$), larger tumor size ($p = 0.0092$), more frequent IMs ($p = 0.0214$), a higher Ki-67 labeling index (LI; $p = 0.0002$), and more Bcl-XL-positive cells ($p = 0.0001$) than the pSTAT3-negative group, whereas no significant differences were noted with respect to sex, age, infection of hepatitis viruses, liver cirrhosis, PIVKA II (proteins induced by vitamin K absence or antagonist II), histological differentiation, capsule formation, infiltration to the capsule, and vessel invasion.

Survival Analysis after Surgery

The median follow-up period was 1,391 days (range 36–3,289). pSTAT3 expression was significantly correlated with OS and DFS ($p = 0.0234$ and 0.0003, respectively; fig. 1d, e). Univariate analyses indicated that high AFP (>100 ng/ml), large tumor size (>5 cm), PVIs and IMs were prognostic factors for OS and male sex, hepatitis C virus infection, high AFP (>100 ng/ml) and IMs for DFS (table 2). Multivariate proportional hazard models revealed that high AFP and IMs were independent prognostic factors for OS and pSTAT3 expression and high AFP for DFS (table 2).

Tumor-Associated Macrophage Localization and pSTAT3 Expression of HCCs

CD163-positive cells were localized around the pSTAT3-positive HCC cells (fig. 2a). Figure 2b shows the boxplots of CD163-positive cells (mean ± SD: pSTAT3-negative group, 28.5 ± 15.4; pSTAT3-positive group, 42.6 ± 26.6). The pSTAT3-positive group (n = 36) showed statistically higher CD163-positive cells ($p = 0.0013$; fig. 2b) than the pSTAT3-negative group (n = 65). Furthermore, we analyzed the localization of CD163-posi-

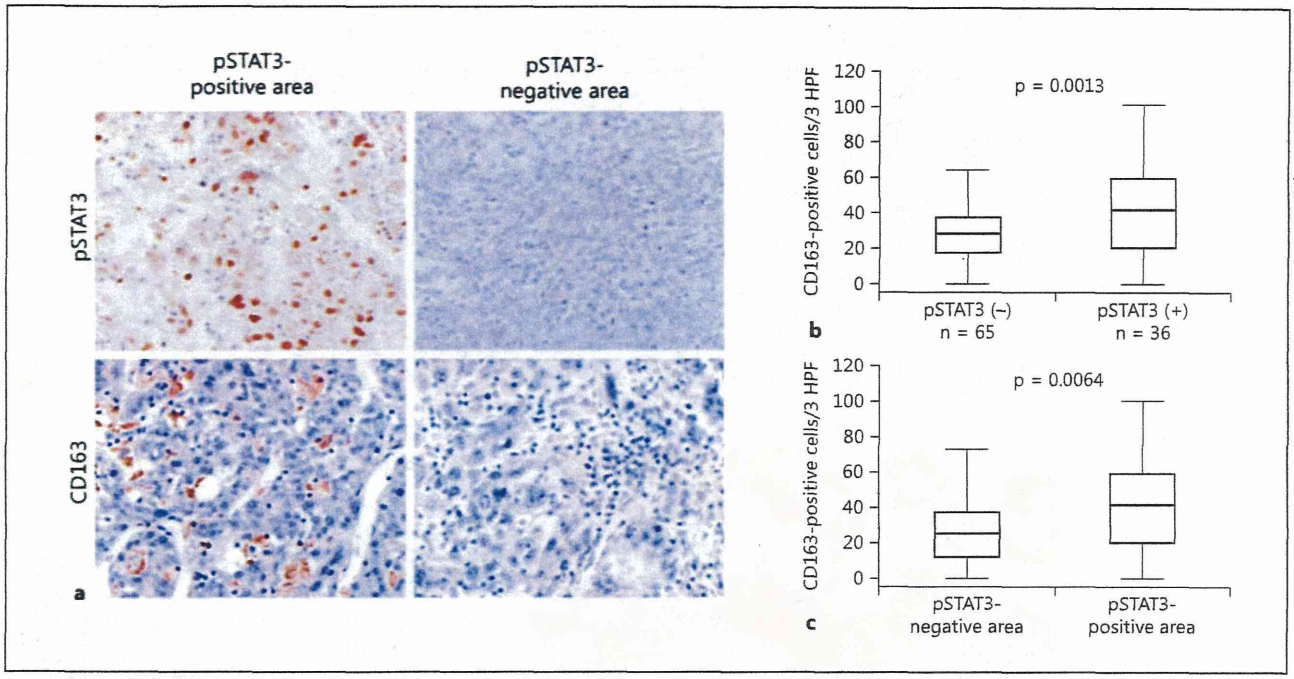

Fig. 2. Tumor-associated macrophages correlated with pSTAT3 expression in HCC. **a** Immunohistochemical staining of pSTAT3 and CD163 in the pSTAT3-positive and pSTAT3-negative area. ×200. **b** Counts of CD163-positive cells between pSTAT3-positve and pSTAT3-negative groups. **c** Counts of CD163-positive cells in areas of pSTAT3-positive and pSTAT3-negative HCC cells existed in the pSTAT3-positive group. HPF = High-power field.

Table 2. Survival analysis after surgery

Variable	Univariate analysis of OS	Multivariate analysis of OS		
	p value	hazard ratio	95% CI	p value
pSTAT3 positive	0.0234*	1.104	0.465–2.683	0.8236
AFP >100 ng/ml	0.0005*	2.968	1.294–7.026	0.0103*
Tumor size >5 cm	0.0246*	1.489	0.610–3.578	0.3755
Portal venous invasion	0.0422*	1.568	0.629–4.1265	0.3367
Intrahepatic metastasis	0.0022*	2.668	1.186–6.194	0.0177*
Variable	Univariate analysis of DFS	Multivariate analysis of DFS		
	p value	hazard ratio	95% CI	p value
pSTAT3 positive	0.0003*	1.851	1.066–3.201	0.0288*
Sex, male	0.0267*	0.978	0.515–1.790	0.9431
HCV Ab (+)	0.0158*	1.672	0.948–3.096	0.0767
AFP >100 ng/ml	0.0002*	2.070	1.218–3.476	0.0076*
Intrahepatic metastasis	0.0012*	1.702	0.964–3.012	0.0664

CI = Confidence interval; HCV Ab = hepatitis C virus antibody. * $p < 0.05$.

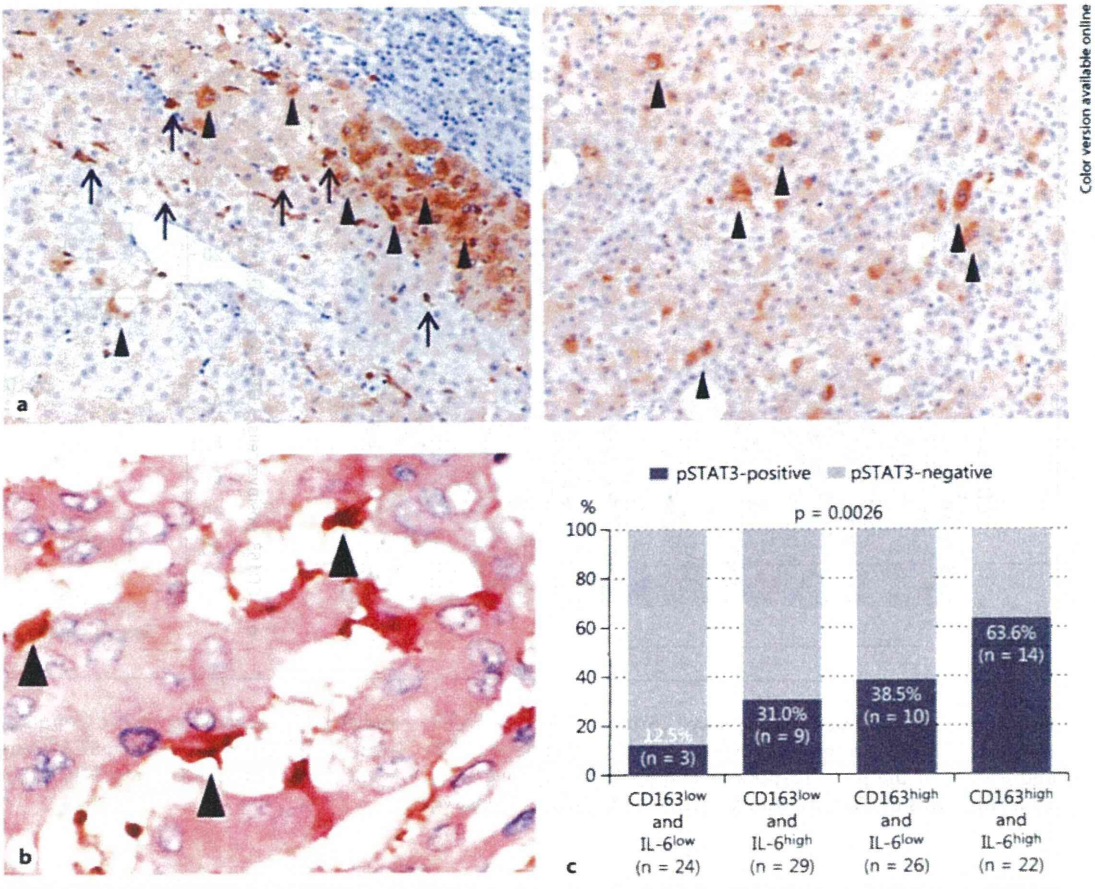

Fig. 3. Tumor-associated macrophages expressed IL-6. **a** Immunohistochemical staining of IL-6 in HCC. ×200. Not only macrophages (arrows, left panel) but also some hepatocytes (arrowheads, left panel) and some tumor cells (arrowheads, right panel) showed immunoreactivities for IL-6. **b** Double staining of IL-6 (red) and CD163 (brown). ×400. Double-positive cells (arrowheads) were frequently seen in the tumor. **c** Correlation between pSTAT3-positive and IL-6/CD163-positive staining.

tive cells in areas where pSTAT3-positive and pSTAT3-negative HCC cells existed in the pSTAT3-positive group (n = 36), and figure 2c shows the boxplots of the analyses (mean ± SD: pSTAT3-negative area, 27.7 ± 17.9; pSTAT3-positive area, 42.6 ± 26.6). In the pSTAT3-positive group, CD163-positive cells in areas where pSTAT3-positive HCC cells existed were statistically higher than in those where pSTAT3-negative HCC cells existed (p = 0.0064; fig. 2c).

Cytokine Expression of Macrophages

IL-6 was stained in some macrophages, HCC cells and normal hepatocytes (fig. 3a). According to the double staining of CD163 and IL-6, CD163-positive cells (tumor-associated macrophages) expressed IL-6 (fig. 3b). We divided them into two by the median values of positive macrophages of IL-6 and CD163, and thereby classified the 101 cases into four groups such as $CD163^{low}$ and $IL\text{-}6^{low}$, $CD163^{low}$ and $IL\text{-}6^{high}$, $CD163^{high}$ and $IL\text{-}6^{low}$, and $CD163^{high}$ and $IL\text{-}6^{high}$. HCCs containing high infiltration of IL-6- and CD163-positive macrophages exhibited a significantly higher rate of positive staining for pSTAT3 (fig. 3c).

IL-6 Stimulates Cell Proliferation and Migration of Human HCC Cell Lines

IL-6 stimulation increased the levels of pSTAT3 in both PLC/PRF/5 and Huh7 HCC cell lines (fig. 4a). IL-6 stimulation resulted in higher proliferation (fig. 4b) and greater migration distance (fig. 4c) versus control. S3I-

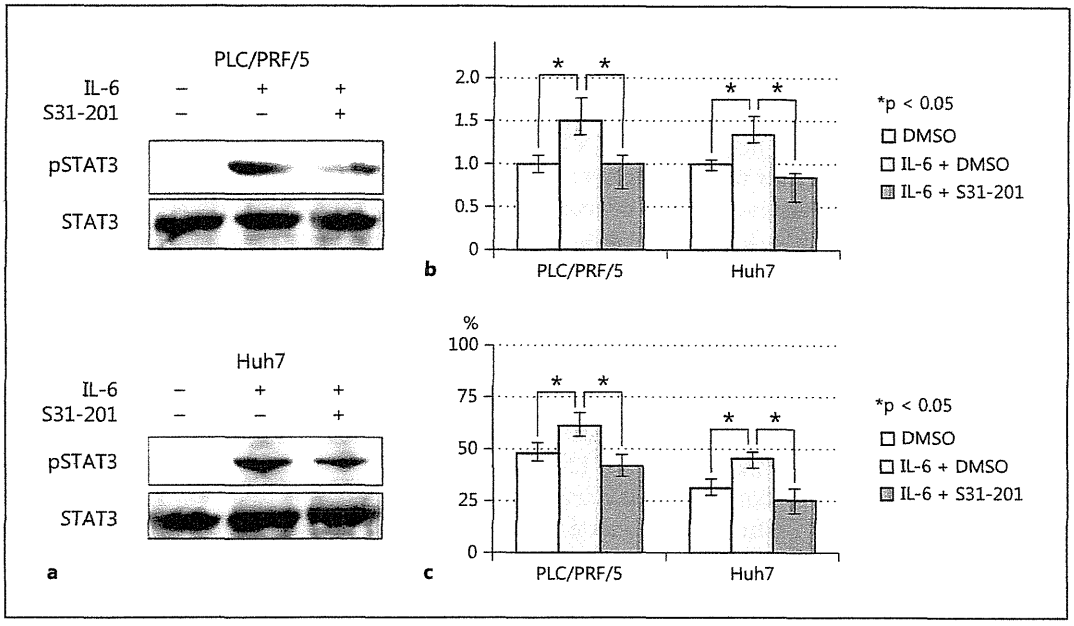

Fig. 4. IL-6 stimulation activated STAT3 signaling and promoted cell proliferation and migration in HCC cell lines. **a** PLC/PRF/5 (upper panel) and Huh7 (lower panel) were treated with 25 ng/ml IL-6 for 30 min. **b** PLC/PRF/5 and Huh7 were cultured with 25 ng/ml IL-6, 100 nM S3I-201 and conditioned medium (1% FBS); cell proliferation was evaluated 48 h after IL-6 stimulation. Control set at 1. **c** PLC/PRF/5 and Huh7 were cultured with 25 ng/ml IL-6, 100 nM S3I-201 and conditioned medium (1% FBS), and wound-healing assay was evaluated 48 h thereafter.

201, a STAT3 inhibitor, inhibited IL-6-induced STAT3 phosphorylation (fig. 4a) and decreased proliferation and migration of HCC cell lines (fig. 4b, c).

Discussion

Our results suggest that macrophage infiltration into HCC tissue stimulates tumor cells via STAT3 signaling. In the present study, pSTAT3-positive HCCs show malignant behavior and confer poor prognosis because of their high abilities of cell proliferation and migration. We found that high pSTAT3 expression was significantly correlated with larger tumor size, higher Ki-67 LI, higher Bcl-XL expression and greater frequency of IMs, and higher pSTAT3 expression was observed in the lesions of IMs and PVIs than in the primary lesions. STAT3 activation upregulates cell cycle-related, antiapoptotic and invasion genes [8–13, 26, 27]. In our results, large tumor size and high Ki-67 LI indicated cell cycle progression, high Bcl-XL expression indicated antiapoptotic function, and frequent IMs indicated invasive capacity. Furthermore, high pSTAT3 expression in the lesions of IMs and PVIs suggests that the tumor cells with STAT3 activation in the primary lesions tended to invade the vessels and metastasize to the other liver sites. Xie et al. [26, 27] reported that activated STAT3 regulated tumor invasion of melanoma cells by regulating the gene transcription of matrix metalloproteinase 2. These results suggest that pSTAT3 expression plays an important role for cell survival and migration in HCC, consistent with previous studies in HCC [14, 17, 28, 29] and other tumors [5, 8–12, 26, 27, 30].

In recent years, it has been recognized that the balance between tumor immunity and tumor progression is important [31]. The present study revealed that tumor-associated macrophages are important for pSTAT3 expression of tumor cells. First, CD163-positive cells around pSTAT3-positive HCC cells were statistically more prevalent than around pSTAT3-negative HCC cells. Some of the CD163-positive cells expressed IL-6 in HCC tissue, and STAT3 was phosphorylated by IL-6 stimulation in vitro. These results suggest that tumor-associated macrophages can activate HCC cells via STAT3 signaling by IL-6 expression. However, CD-163-positive cells were detected not only in the pSTAT3-negative tumor area but

also in the pSTAT3-positive tumor area and in noncancerous liver tissue. IL-6-secreting tumor-associated macrophages may be part of the CD163-positive cells, and the CD163-positive cells in the pSTAT3-positive tumor area were more stained by IL-6 than in the pSTAT3-negative tumor area and normal liver tissue (data not shown). Tumor-associated macrophages express immunosuppressive cytokines including IL-4, IL-6, IL-10, IL-17, and IL-23 [32, 33]. These cytokines activate immunosuppressive inflammatory cells such as other tumor-associated macrophages, helper T cells and regulatory T cells and suppress antitumor inflammatory cells such as lymphocytes, natural killer cells and dendritic cells [34–36]. Kuang et al. [32] showed that tumor-associated macrophages expressed IL-6 in vitro, whereas Ding et al. [21] reported that tumor-associated macrophage was correlated with poor prognosis in HCC. Our results are consistent with these previous reports.

Both proliferation and migration of PLC/RPF/5 and Huh7 were increased following IL-6 stimulation and STAT3 phosphorylation. On the other hand, IL-6 was expressed in not only macrophages but also in HCC cells. STAT3 can be activated through autocrine signaling in HCC cells; moreover, other cytokines and growth factors might activate STAT3 of tumor cells [22–24]. It is very difficult to exclude activation of STAT3 by the autocrine manner. In our data, STAT3 activation of HCC cells was not correlated with surrounding IL-6-positive normal hepatocytes and HCC cells but it was correlated with the infiltration of CD-163-positive cells (fig. 2). Thus, we thought that the IL-6 secretion of tumor-associated macrophages is more important for STAT3 activation of HCC cells than the IL-6 secretion of other cells.

Recently, STAT3 phosphorylation inhibitors such as S3I-201 have been investigated in vitro and in vivo [28–30]. Avella et al. [37] reported that STAT3 can be one of the targets of chemoimmunotherapies. In our study, S3I-201 inhibited IL-6-induced STAT3 phosphorylation in vitro and decreased cell proliferation and migration. The inhibition of tumor-associated macrophages as therapeutic strategy of malignancy has been investigated, too [38–41]. Therefore, it is very important to suppress tumor-associated macrophage activation and STAT3 signaling in the treatment of HCC. Furthermore, tumor-associated macrophage activation requires STAT3 signaling [22]. We consider that the STAT3 inhibitor may suppress STAT3 activation in both tumor cells and tumor-associated macrophages, release antitumor immune systems from suppression by tumor-associated macrophages and thereby control tumor progression of HCC. Therefore, STAT3 signaling is a feasible therapeutic target for HCC.

In conclusion, STAT3 activation is one of the prognostic factors in HCC. Tumor-associated macrophage expresses IL-6 and can activate STAT3 signaling of HCC cells, resulting in their cell proliferation, antiapoptosis and migration. In the future, HCC may be suppressed by inhibition of STAT3 signaling of tumor cells and tumor-associated macrophages.

Disclosure Statement

The authors have no conflicts of interest.

References

1 Llovet JM, Burroughs A, Bruix J: Hepatocellular carcinoma. Lancet 2003;362:1907–1917.
2 Shirabe K, Kanematsu T, Matumata T, Adachi E, Akazawa K, Sugimachi K: Factors linked to early recurrence of small hepatocellular carcioma after hepatectomy: univariate and multivariate analyses. Hepatology 1991; 14:802–805.
3 Taura K, Ikai I, Hatano E, Fujii H, Uyama N, Shimahara Y: Implication of frequent local ablation therapy for intrahepatic recurrence in prolonged survival of patients with hepatocellular carcinoma undergoing hepatic resection: an analysis of 610 patients over 16 years old. Ann Surg 2006;244:265–273.
4 Llovet JM, Ricci S, Mazzaferro V, Hilgard P, Gane E, Blanc JF, de Oliveira AC, Santoro A, Raoul JL, Forner A, Schwartz M, Porta C, Zeuzem S, Bolondi L, Greten TF, Galle PR, Seitz JF, Borbath I, Häussinger D, Giannaris T, Shan M, Moscovici M, Voliotis D, Bruix J, SHARP Investigators Study Group: Sorafenib in advanced hepatocellular carcinoma. N Engl J Med 2008;359:378–390.
5 Bromberg JF, Wrzeszczynska MH, Devgan G, Zhao Y, Pestell RG, Albanese C, Darnell JE Jr: Stat3 as an oncogene. Cell 1999;98:295–303.
6 Al Zaid Siddiquee K, Turkson J: STAT3 as a target for inducing apoptosis in solid and hematological tumors. Cell Res 2008;18:254–267.
7 Murray PJ: The JAK-STAT signaling pathway: input and output integration. J Immunol 2007;178:2623–2629.
8 Berishaj M, Gao SP, Ahmed S, Leslie K, Al-Ahmadie H, Gerald WL, Bornmann W, Bromberg JF: Stat3 is tyrosine-phosphorylated through the interleukin-6/glycoprotein 130/Janus kinase pathway in breast cancer. Breast Cancer Res 2007;9:R32.

9 Lin Q, Lai R, Chirieac LR, Li C, Thomazy VA, Grammatikakis I, Rassidakis GZ, Zhang W, Fujio Y, Kunisada K, Hamilton SR, Amin HM: Constitutive activation of JAK3/STAT3 in colon carcinoma tumors and cell lines: inhibition of JAK3/STAT3 signaling induces apoptosis and cell cycle arrest of colon carcinoma cells. Am J Pathol 2005;167:969–980.
10 Song L, Turkson J, Karras JG, Jove R, Haura EB: Activation of Stat3 by receptor tyrosine kinases and cytokines regulates survival in human non-small cell carcinoma cells. Oncogene 2003;22:4150–4165.
11 Greten FR, Weber CK, Greten TF, Schneider G, Wagner M, Adler G, Schmid RM: Stat3 and NF-kappaB activation prevents apoptosis in pancreatic carcinogenesis. Gastroenterology 2002;123:2052–2063.
12 Ni Z, Lou W, Leman ES, Gao AC: Inhibition of constitutively activated Stat3 signaling pathway suppresses growth of prostate cancer cells. Cancer Res 2000;60:1225–1228.
13 Kreis S, Munz GA, Haan S, Heinrich PC, Behrmann I: Cell density dependent increase of constitutive signal transducers and activators of transcription 3 activity in melanoma cells is mediated by Janus kinases. Mol Cancer Res 2007;5:1331–1341.
14 Rajendran P, Ong TH, Chen L, Li F, Shanmugam MK, Vali S, Abbasi T, Kapoor S, Sharma A, Kumar AP, Hui KM, Sethi G: Suppression of signal transducer and activator of transcription 3 activation by butein inhibits growth of human hepatocellular carcinoma in vivo. Clin Cancer Res 2011;17:1425–1439.
15 Yang SF, Wang SN, Wu CF, Yeh YT, Chai CY, Chunag SC, Sheen MC, Lee KT: Altered p-STAT3 (Tyr705) expression is associated with histological grading and intratumour microvessel density in hepatocellular carcinoma. J Clin Pathol 2007;60:642–648.
16 Ogata H, Kobayashi T, Chinen T, Takaki H, Sanada T, Minoda Y, Koga K, Takaesu G, Maehara Y, Iida M, Yoshimura A: Deletion of the SOCS3 gene in liver parenchymal cells promotes hepatitis-induced hepatocarcinogenesis. Gastroenterology 2006;131:179–193.
17 Pollard JW: Tumour-educated macrophages promote tumour progression and metastasis. Nat Rev Cancer 2004;4:71–78.
18 Lewis CE, Pollard JW: Distinct role of macrophages in different tumor microenvironments. Cancer Res 2006;66:605–612.
19 Hasita H, Komohara Y, Okabe H, Masuda T, Ohnishi K, Lei XF, Beppu T, Baba H, Takeya M: Significance of alternatively activated macrophages in patients with intrahepatic cholangiocarcinoma. Cancer Sci 2010;101:1913–1919.
20 Siveen KS, Kuttan G: Role of macrophages in tumor progression. Immunol Letter 2009;123:97–102.
21 Ding T, Xu J, Wang F, Shi M, Zhang Y, Li SP, Zheng L: High tumor-infiltrating macrophage density predicts poor prognosis in patients with primary hepatocellular carcinoma after resection. Hum Pathol 2009;40:381–389.
22 Fujiwara Y, Komohara Y, Ikeda T, Takeya M: Corosolic acid inhibits glioblastoma cell proliferation by suppressing the activation of signal transducer and activator of transcription-3 and nuclear factor-kappa B in tumor cells and tumor-associated macrophages. Cancer Sci 2011;102:206–211.
23 Takaishi K, Komohara Y, Tashiro H, Ohtake H, Nakagawa T, Katabuchi H, Takeya M: Involvement of M2-polarized macrophages in the ascites from advanced epithelial ovarian carcinoma in tumor progression via Stat3 activation. Cancer Sci 2010;101:2128–2136.
24 Domínguez-Soto A, Sierra-Filardi E, Puig-Kröger A, Pérez-Maceda B, Gómez-Aguado F, Corcuera MT, Sánchez-Mateos P, Corbí AL: Dendritic cell-specific ICAM-3-grabbing nonintegrin expression on M2-polarized and tumor-associated macrophages is macrophage-CSF dependent and enhanced by tumor-derived IL-6 and IL-10. J Immunol 2011;186:2192–2200.
25 Komohara Y, Ohnishi K, Kuratsu J, Takeya M: Possible involvement of the M2 anti-inflammatory macrophage phenotype in growth of human gliomas. J Pathol 2008;216:15–24.
26 Xie TX, Wei D, Liu M, Gao AC, Ali-Osman F, Sawaya R, Huang S: Stat3 activation regulates the expression of matrix metalloproteinase-2 and tumor invasion and metastasis. Oncogene 2004;23:3550–3560.
27 Xie TX, Huang FJ, Aldape KD, Kang SH, Liu M, Gershenwald JE, Xie K, Sawaya R, Huang S: Activation of Stat3 in human melanoma promotes brain metastasis. Cancer Res 2006;66:3188–3196.
28 Lin L, Amin R, Gallicano GI, Glasgow E, Jogunoori W, Jessup JM, Zasloff M, Marshall JL, Shetty K, Johnson L, Mishra L, He AR: The STAT3 inhibitor NSC 74859 is effective in hepatocellular cancers with disrupted TGF-beta signaling. Oncogene 2009;28:961–972.
29 Choudhari SR, Khan MA, Harris G, Picker D, Jacob GS, Block T, Shailubhai K: Deactivation of Akt and STAT3 signalling promotes apoptosis, inhibits proliferation, and enhances the sensitivity of hepatocellular carcinoma cells to an anticancer agent, Atiprimod. Mol Cancer Ther 2007;6:112–121.
30 Lin L, Hutzen B, Zuo M, Ball S, Deangelis S, Foust E, Pandit B, Ihnat MA, Shenoy SS, Kulp S, Li PK, Li C, Fuchs J, Lin J: Novel STAT3 phosphorylation inhibitors exhibit potent growth-suppressive activity in pancreatic and breast cancer cells. Cancer Res 2010;70:2445–2454.
31 Korangy F, Höchst B, Manns MP, Greten TF: Immune responses in hepatocellular carcinoma. Dig Dis 2010;28:150–154.
32 Kuang DM, Peng C, Zhao Q, Wu Y, Chen MS, Zheng L: Activated monocytes in peritumoral stroma of hepatocellular carcinoma promote expansion of memory T helper 17 cells. Hepatology 2010;51:154–164.
33 Kortylewski M, Xin H, Kujawski M, Lee H, Liu Y, Harris T, Drake C, Pardoll D, Yu H: Regulation of the IL-23 and IL-23 balance by Stat3 signaling in the tumor microenvironment. Cancer Cell 2009;15:114–123.
34 Kuang DM, Zhao Q, Peng C, Xu J, Zhang JP, Wu C, Zheng L: Activated monocytes in peritumoral stroma of hepatocellular carcinoma foster immune privilege and disease progression through PD-L1. J Exp Med 2009;206:1327–1337.
35 Wu K, Kryczek I, Chen L, Zou W, Welling TH: Kupffer cell suppression of CD8+ T cells in human hepatocellular carcinoma is mediated by B7-H1/programmed death-1 interactions. Cancer Res 2009;69:8067–8075.
36 Niemand C, Nimmesgern A, Haan S, Fischer P, Schaper F, Rossaint R, Heinrich PC, Müller-Newen G: Activation of STAT3 by IL-6 and IL-10 in primary human macrophages is differentially modulated by suppressor of cytokine signaling 3. J Immunol 2003;170:3263–3272.
37 Avella DM, Li G, Schell TD, Liu D, Zhang SS, Lou X, Berg A, Kimchi ET, Tagaram HR, Yang Q, Shereef S, Garcia LS, Kester M, Isom HC, Rountree CB, Staveley-O'Carroll KF: Regression of established hepatocellular carcinoma is induced by chemoimmunotherapy in an orthotopic murine model. Hepatology 2012;55:141–152.
38 Zhang W, Zhu XD, Sun HC, Xiong YQ, Zhuang PY, Xu HX, Kong LQ, Wang L, Wu WZ, Tang ZY: Depletion of tumor-associated macrophages enhances the effect of sorafenib in metastatic liver cancer models by antimetastatic and antiangiogenic effects. Clin Cancer Res 2010;16:3420–3430.
39 Luo Y, Zhou H, Krueger J, Kaplan C, Lee SH, Dolman C, Markowitz D, Wu W, Liu C, Reisfeld RA, Xiang R: Targeting tumor-associated macrophages as a novel strategy against breast cancer. J Clin Invest 2006;116:2132–2141.
40 Huang Y, Snuderl M, Jain RK: Polarization of tumor-associated macrophages: a novel strategy for vascular normalization and antitumor immunity. Cancer Cell 2011;19:1–2.
41 Wu WY, Li J, Wu ZS, Zhang CL, Meng XL: STAT3 activation in monocytes accelerates liver cancer progression. BMC Cancer 2011;11:506.

IJC
International Journal of Cancer

The combination therapy of α-galactosylceramide and 5-fluorouracil showed antitumor effect synergistically against liver tumor in mice

Hiroshi Aketa[1]*, Tomohide Tatsumi[1]*, Keisuke Kohga[2], Hinako Tsunematsu[1], Satoshi Aono[1], Satoshi Shimizu[1], Takahiro Kodama[1], Takatoshi Nawa[1], Minoru Shigekawa[1], Hayato Hikita[1], Ryotaro Sakamori[1], Atsushi Hosui[1], Takuya Miyagi[1], Naoki Hiramatsu[1], Tatsuya Kanto[1], Norio Hayashi[1,3] and Tetsuo Takehara[1]

[1] Department of Gastroenterology and Hepatology, Osaka University Graduate School of Medicine, Suita, Osaka, Japan
[2] Kohga Hospital, Yaizu, Shizuoka, Japan
[3] Kansai-Rosai Hospital, Amagasaki, Hyogo, Japan

α-Galactosylceramide (α-GalCer) has been reported to be therapeutic against metastatic liver tumors in mice. However, little is known regarding the efficacy of combined chemo-immunotherapy using α-GalCer and anticancer drugs. In this study, we evaluated the antitumor effect of the combination therapy of α-GalCer and 5-fluorouracil (5-FU) against liver tumors of MC38 colon cancer cells. The liver weights of tumor-bearing mice treated with the combination were significantly lower than those of nontreated mice and of mice treated with 5-FU or α-GalCer alone. No toxic effects on the liver and renal functions were observed in any of the treatment groups. α-GalCer treatment induced significant activation of liver NK cells *in vivo*, but 5-FU treatment did not. 5-FU treatment resulted in a significant upregulation of NKG2D activating molecules (Rae-1 and H60) and DNAM-1 ligands (CD112 and CD155) on MC38 cells, but α-GalCer did not. The cytolytic activity of α-GalCer-activated liver mononuclear cells against 5-FU-treated MC38 cells was significantly higher than that against nontreated cells. The increase of the cytolytic activity induced by 5-FU partially depended on NKG2D-Rae-1 or H60 signals. Depletion of NK cells significantly inhibited the antitumor efficacy of 5-FU against MC38 liver tumors, which suggested that the antitumor effect of 5-FU partially depended on the cytolytic activity of NK cells. These results demonstrated that the combination therapy of α-GalCer and 5-FU produced synergistic antitumor effects against liver tumors by increasing the expression of NK activating molecules on cancer cells. This study suggests a promising new chemo-immunotherapy against metastatic liver cancer.

Colon cancer is one of the most common cancers in the world. Despite recent progress in the development of treatment, the overall 5-year survival rate is only 50–60% due to local recurrence or distant metastasis.[1] In particular, patients with metastatic colon cancer have a median survival rate of only six months. 5-Fluorouracil (5-FU) remains key-drug in chemotherapy against colon cancer. However, colon cancer cells are becoming increasingly resistant to existing chemotherapies including 5-FU.[2] Therefore, novel strategies are needed especially for the treatment of advanced colon cancers including metastatic liver cancer.

A normal liver contains abundant lymphocytes that are usually enriched with NK and NKT cells in contrast to peripheral blood.[3,4] Thus, the effective activation of innate immune cells might be beneficial in the treatment of metastatic liver cancer. To date, however, immunotherapy has not yet been established against metastatic liver cancer. α-Galactosylceramide (α-GalCer) induces the activation of NKT cells in a CD1d-dependent manner.[5,6] Recently, α-GalCer has been attracting attention as a novel antitumor therapy. Systemic administration of α-GalCer has demonstrated antitumor effects against various tumors (including melanoma, sarcoma, colon carcinoma, and lymphoma) *in vivo* in animal models of hepatic and lung metastasis.[7,8] We and others have demonstrated that sequential activation of both NKT and NK cells could be observed in the liver after α-GalCer administration.[8–10] Although most NKT cells had disappeared from the liver within 12 hr of α-GalCer administration, strong activation and proliferation of liver NK cells could be

Key words: α-GalCer, 5-FU, NK cells, liver tumor

Abbreviations: 5-FU: 5-fluorourcil; Alb: albumin; ALT: alanine aminotransferase; Cr: creatinine; IFN-α: interferon-α; MICA: major histocompatibility complex class I-related chain A; MNCs: mononuclear cells; PBS: phosphate buffered saline; T-Bil: total bilirubin; α-GalCer: α-galactosylceramide

*H.A. and T.T. contributed equally to this work and share the first authorship.

Grant sponsor: Ministry of Education, Culture, Sports, Science and Technology of Japan, Research on Hepatitis, Ministry of Health, Labour and Welfare of Japan (BSE)
DOI: 10.1002/ijc.28118
History: Received 20 July 2012; Accepted 29 Jan 2013; Online 19 Feb 2013

Correspondence to: Tomohide Tatsumi, Department of Gastroenterology and Hepatology, Osaka University Graduate School of Medicine, 2-2 Yamadaoka, Suita, Osaka 565-0871, Japan, Fax: +81-6-6879-3629, E-mail: tatsumit@gh.med.osaka-u.ac.jp

What's new?
α-Galactosylceramide (α-GalCer) is effective against metastatic liver tumors in mice. In this study, the authors evaluated the antitumor effect of a combination therapy of α-GalCer plus 5-FU. They found that the combination therapy produced synergistic antitumor effects against liver tumors of colon cancer cells in mice, by both increasing the activation of natural killer (NK) cells and enhancing the sensitivity of the cancer cells to those NK cells. This combination may therefore represent a promising new chemo-immunotherapy against metastatic liver cancer.

observed, and the antitumor effect of the α-GalCer treatment against liver tumors depended primarily on NK cells. Based on the promising results of preclinical studies, several Phase 1 clinical studies using intravenous administration of α-GalCer have been conducted, but clinical responses of α-GalCer have been limited.[11] In view of future α-GalCer treatment of metastatic liver cancer, new strategies should be explored. We have previously reported that anticancer drugs enhance the expression of the human NKG2D ligand, membrane-bound major histocompatibility complex class I-related chain A (MICA), and the NK sensitivity of human hepatocellular carcinoma cells *in vitro*.[12,13] These findings suggest that the efficient activation of liver innate immunity after chemotherapy might represent a promising approach to the suppression of liver tumor growth.

In this study, we investigated the therapeutic potential of the combination of α-GalCer and 5-FU in the treatment of liver tumor of colon cancer cells. We found that 5-FU can enhance the NK sensitivity of colon cancer cells by increasing the expression of NK activating molecules. In addition, the combination therapy of α-GalCer and 5-FU showed synergistic antitumor effects against liver tumor of colon cancer cells. This study demonstrates a promising new therapeutic strategy for the treatment of metastatic liver cancer.

Material and Methods

Mice

Female C57BL/6 and BALB/c mice were purchased from Charles River Laboratories Japan, INC (Yokohama, Japan) and were used at 6–10 weeks of age. The mice were housed under conditions of controlled temperature and light with free access to food and water at the Institute of Experimental Animal Science, Osaka University Graduate School of Medicine. All animals received humane care and our study protocol complied with the institution's guidelines.

Cell lines

MC38, a mouse colon cancer cell line derived from C57BL/6 mice, was generously provided by Dr. Michio Imawari (Showa University School of Medicine, Tokyo, Japan). Colon26, a mouse colon cancer cell line derived from BALB/c mice, was kindly provided by Dr. Takashi Tsuruo (Institute of Molecular and Cellular Bioscience, University of Tokyo, Tokyo, Japan). This cell line was maintained in complete medium (CM, RPMI-1640 medium supplemented with 10% heat-inactivated fetal bovine serum, 100 U/ml penicillin, 100 μg/ml streptomycin, and 10 mM L-glutamine: all reagents from GIBCO/Life Technologies, Grand Island, NY) in a humidified incubator at 5% CO_2 and 37°C.

Reagents

α-GalCer was purchased from Funakoshi (Tokyo, Japan) and prepared as previously described by Kawano *et al.*[5] 5-FU was purchased from Kyowa Hakko Kirin (Tokyo, Japan) and dissolved in phosphate buffered saline (PBS). MC38 cell viability was determined 24 hr after the addition of 5-FU (used at 10 nmol/l to 2 μmol/l) or PBS by the WST assay using the cell count reagent SF (Nacalai Tesque, Kyoto, Japan) as previously described (10).

Flow cytometry

MC38 cells were cultured with or without α-GalCer (100 ng/ml) or 5-FU (500 nmol/l) for 24 hr and evaluated for the expression of NK activating molecules. Treated and non-treated MC38 cells were incubated with PE-conjugated antibodies (Abs) against anti-Rae-1 (R&D Systems, Minneapolis, MN), H60 (R&D Systems), CD112 (Nectin-2) (Abcam, Cambridge, UK), and CD155 (BioLegend, San Diego, CA). Flow cytometric analysis was performed using a Canto II flow cytometer (Becton Dickinson, San Jose, CA).

Preparation of hepatic mononuclear cells from 5-FU- or α-GalCer-treated mice

C57BL/6 mice were administered 5-FU (20 mg/kg body weight)or PBS intraperitoneally (i.p.) for 3 consecutive days. Liver mononuclear cells (MNCs) were prepared as previously described.[8] In some experiments, C57BL/6 mice were administered α-GalCer (0.4 μg/mouse) or PBS i.p. on Day 0. On Day 3, hepatic MNCs were prepared. NK cells were identified as DX5+/TCRβ- by flow cytometry as previously described.[8] The expression levels of NKG2D and DNAM1 were evaluated with anti-NKG2D (R&D Systems) and anti-DNAM1 (BioLegend) Abs by flow cytometry.

Cytolytic assays

C57BL/6 mice were injected i.p. with α-GalCer (2 μg/mouse) for the preparation of activated NK cells as previously described.[8] Liver MNCs were prepared on Day 3 after α-GalCer injection. MC38 cells were cultured with or without 5-FU (500 nmol/l) for 1 day. α-GalCer-activated liver MNCs

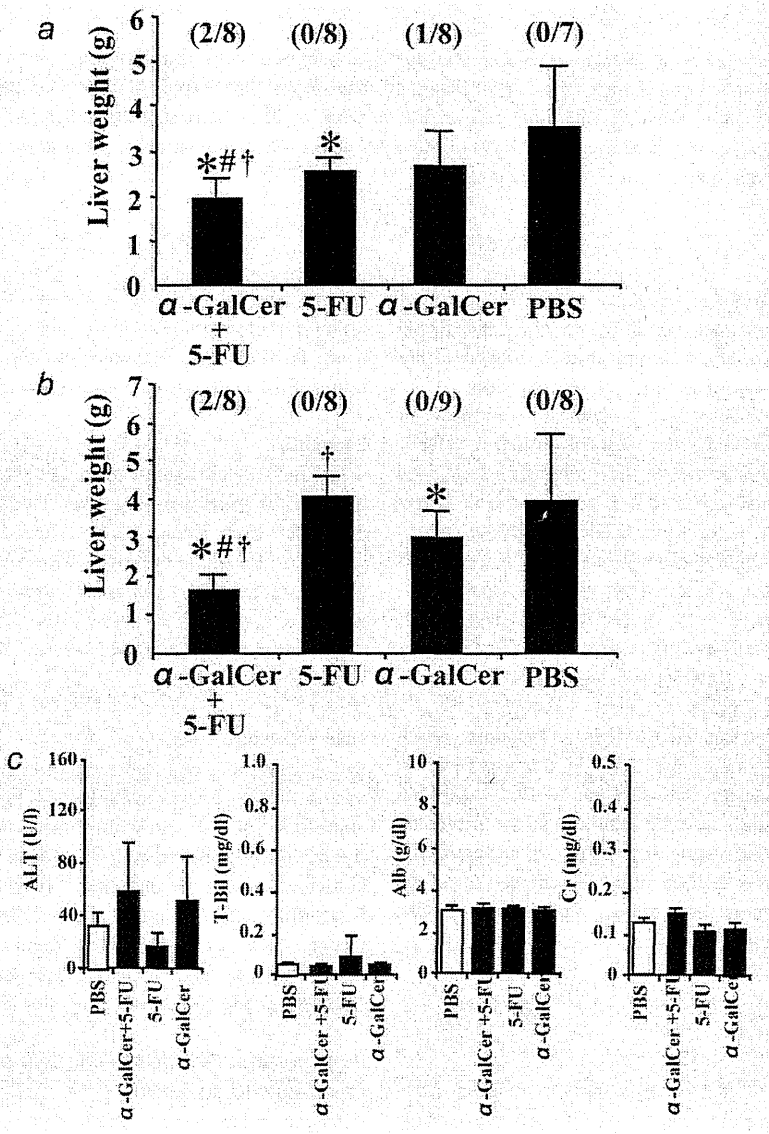

Figure 1. The antitumor effect of the α-GalCer and 5-FU combination therapy against MC38 liver tumors. (*a*, *b*) C57BL/6 mice or BALB/c mice were injected in the liver with 3×10^5 MC38 cells or 5×10^5 Colon26 cells on Day 0. To evaluate the efficacy of the α-GalCer and 5-FU combination therapy, the mice were treated with α-GalCer (0.4 μg/mouse) on Day 0 and/or 5-FU (C57BL/6, 10 mg/kg body weight; BALB/c, 20 mg/kg body weight) for 5 consecutive days after tumor inoculation. Two weeks after the tumor injection, the liver weight was measured to examine intrahepatic tumor growth. $N = 7$–9 mice/group. Each data point represents the mean liver weight ± SD. The fraction of mice achieving tumor rejection in each treatment group is shown in parentheses. *$p < 0.05$ *versus* PBS group, #$p < 0.05$ *versus* 5-FU group, †$p < 0.05$ *versus* α-GalCer group. (*c*) Blood samples from treated C57BL/6 mice were obtained 1 day after the final injection of each treatment. The serum levels of ALT, T-Bil, Alb, and Cr were examined. $N = 3$ /group. No significant differences were observed between any of the groups.

were subjected to a 4-hr ^{51}Cr release assay against 5-FU-treated or nontreated MC38 cells as previously described.[12] The assays were performed in triplicate, and the spontaneous release of all assays did not exceed 25% of the maximum release. In some experiments, the cytolytic ability of activated NK cells was assessed by a 4-hr ^{51}Cr-release assay with or without blocking Abs against Rae-1 (R&D Systems) or H60 (R&D Systems).

Animal experiments

C57BL/6 or BALB/c mice were injected in the liver with 3×10^5 MC38 cells or 5×10^5 Colon26 cells on Day 0.

To evaluate the efficacy of the combination therapy of α-GalCer and 5-FU, the mice were treated with α-GalCer (0.4 μg/mouse) on Day 0 and/or 5-FU (C57BL/6, 10 mg/kg body weight; BALB/c, 20 mg/kg body weight respectively) for 5 consecutive days after tumor inoculation. Two weeks after the tumor injection, the liver weight was measured to examine the intrahepatic tumor growth. To evaluate the involvement of NK cells in the antitumor effect of 5-FU, mice were injected with an anti-asialo GM-1 (ASGM1) Ab (WAKO, Osaka, Japan) on Days −1, 4, and 9 after tumor inoculation. The efficiency of NK cell depletion was validated by flow cytometric analysis of splenocytes using PE-conjugated anti-DX5 mAbs (BD-Pharmingen) as previously described.[8] NK-depleted mice were treated with or without 5-FU (10 mg/kg body weight) for 5 consecutive days. Two weeks after the tumor injection, the livers of treated mice were removed, and the liver weight was measured to examine the intrahepatic tumor growth.

NKG2D lignads and DNAM1 ligands expression in MC38 tumor tissues and nontumor tissues in 5-FU-treated mice

C57BL/6 mice were injected in the liver with 3×10^5 MC38 cells on Day 0 and were treated with 5-FU on Day 4–8 after tumor inoculation. On Day 8, MC38 liver tumor or nontumor tissues were harvested and divided into single cells to evaluate the expression of NKG2D ligands (Rae-1 and H60) and DNAM1 ligands (CD112 and CD155) by flow cytometry.

Blood biochemistry test

Blood samples were obtained 24 hr after treatment. The levels of serum alanine aminotransferase (ALT), total bilirubin (T-Bil), albumin (Alb), and creatinine (Cr) were measured with a standard UV method using a Hitachi type 7170 automatic analyzer (Tokyo, Japan).

Statistics

All values are expressed as the mean and SD. Statistical analyses were performed by the unpaired Mann–Whitney *U* test or one-way ANOVA unless otherwise indicated. When ANOVA analyses were applied, differences in the mean values among groups were examined by the Scheffe post hoc correction. We defined statistical significance as $p < 0.05$.

Results

The combination therapy of α-GalCer and 5-FU showed a synergistic antitumor effect against MC38 liver tumors

We examined the antitumor effect of the combination therapy of α-GalCer and 5-FU against MC38 liver tumors. C57BL/6 mice were injected intrahepatically with MC38 cells. The mice were treated with α-GalCer on Day 0 and/or 5-FU for 5 consecutive days after tumor inoculation. As shown in Figure 1*a*, the liver weights of the mice treated with α-GalCer plus 5-FU were significantly lower than those of nontreated mice and mice treated with either 5-FU or α-GalCer alone. The liver weights of mice treated with 5-FU were significantly lower than those of nontreated mice, but treatment with α-GalCer did not produce this effect. We also examined the antitumor effect of α-GalCer plus 5-FU in a Colon26 liver tumor model. The liver weights of mice treated with α-GalCer plus 5-FU were significantly lower than those of nontreated mice and mice treated with either 5-FU or α-GalCer alone. The liver weights of mice treated with α-GalCer were significantly lower than those of nontreated and 5-FU-treated mice (Fig. 1*b*). Tumor rejection in the MC38 liver tumor model was observed in 2/8 of the α-GalCer plus 5-FU-treated

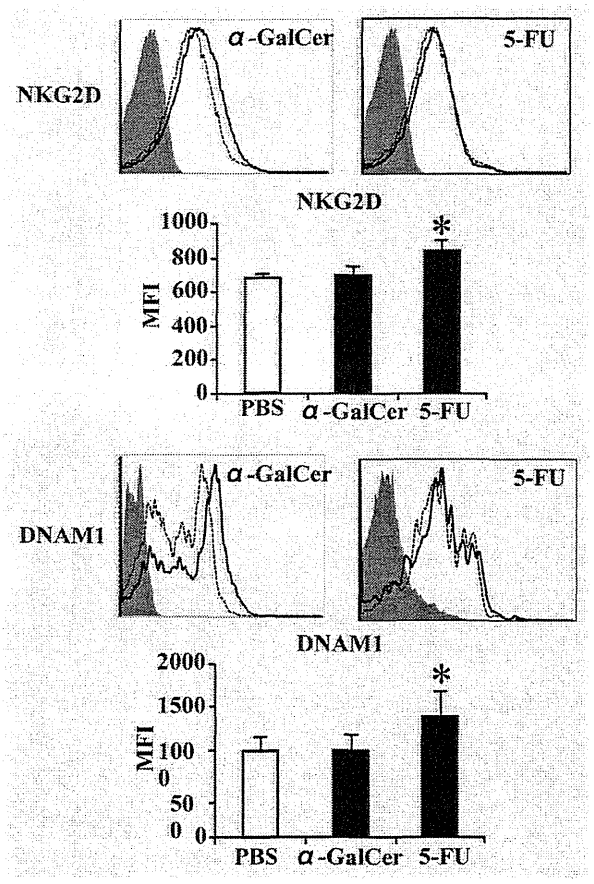

Figure 2. Expression of NKG2D and DNAM1 on liver NK cells isolated from α-GalCer- or 5-FU-treated mice. C57BL/6 mice were treated with α-GalCer (0.4 μg/mouse) i.p. on Day 0 or with 5-FU (10 mg/kg body weight) for 3 consecutive days. Liver NK cells were isolated from α-GalCer or 5-FU-treated mice, and the expression levels of NKG2D and DNAM1 were evaluated by flow cytometry. Black bold line histograms: NKG2D or DNAM1 staining of NK cells from α-GalCer or 5-FU-treated mice; dotted line histograms: NKG2D or DNAM1 staining of NK cells from PBS-treated mice; shaded/gray histograms: control staining. The data are represented as the average of the MFI obtained from 3 separate experiments. *$p < 0.05$ *versus* PBS-treated group.

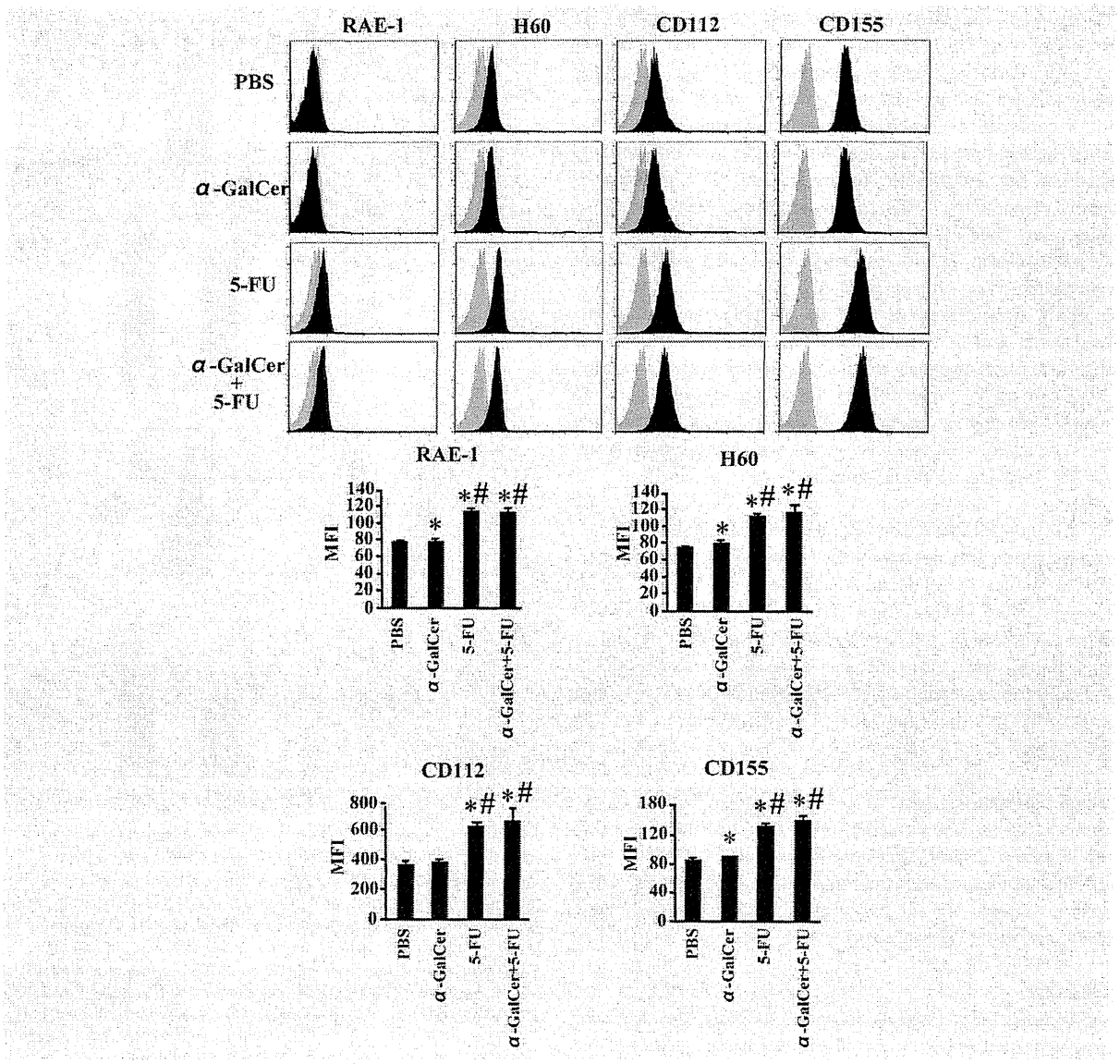

Figure 3. Expression of NKG2D ligands (Rae-1 and H60) and DNAM1 ligands (CD112 and CD155) on MC38 cells treated with α-GalCer and/or 5-FU. MC38 cells were cultured with or without α-GalCer (100 ng/ml) or 5-FU (500 nmol/l) for 24 hr. The treated cells were harvested and evaluated for the expression levels of NKG2D ligands (Rae-1 and H60) and DNAM1 ligands (CD112 and CD155) on MC38 cells by flow cytometry. Upper panel: representative data. Shaded/black histograms: NKG2D or DNAM1 ligand staining of α-GalCer or 5-FU-treated MC38 cells; shaded/gray histograms, control staining. Lower panel: data are represented as the average of MFI obtained from 3 separate experiments. *$p < 0.05$ *versus* PBS group, #$p < 0.05$ *versus* α-GalCer group.

mice, 0/8 of the 5-FU-treated mice, 1/8 of the α-GalCer-treated mice, and 0/7 of the PBS-treated mice (Fig. 1*a*). These results were consistent with those of another Colon26 liver tumor model in BALB/c mice, where tumor rejection was observed in 2/8 of the α-GalCer plus 5-FU-treated mice, 0/8 of the 5-FU-treated mice, 0/9 of the α-GalCer-treated mice, and 0/8 of the PBS-treated mice (Fig. 1*b*). These results demonstrated that the combination therapy of α-GalCer and 5-FU produced a synergistic antitumor effect against liver tumors in both the MC38 and Colon26 models. To evaluate the safety of this combination therapy, serum levels of ALT, T-Bil, Alb, and Cr were evaluated in C57BL/6 mice immunized with α-GalCer plus 5-FU, 5-FU, α-GalCer, or PBS. There was no toxic effect upon the ALT, T-Bil, Alb, or Cr levels for any of the treatment groups (Fig. 1*c*). These results demonstrated that the combination therapy of α-GalCer and

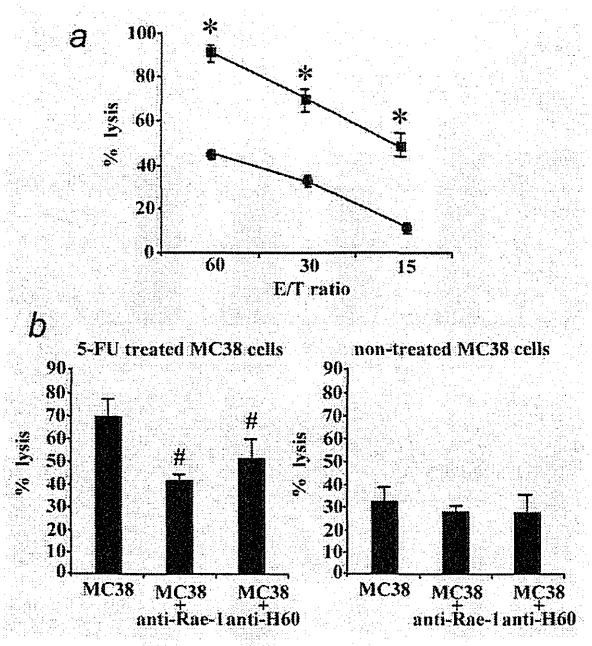

Figure 4. The cytolytic activity of α-GalCer-activated MNCs against 5-FU-treated MC38 cells. C57BL/6 mice were injected i.p. with α-GalCer (2 μg/mice) to activate NK cells. Liver MNCs were prepared on Day 3 after α-GalCer injection. (*a*) MC38 cells were cultured with or without 5-FU (500 nmol/l) for 24 hr. α-GalCer-activated liver MNCs were subjected to a 4-hr ^{51}Cr release assay against 5-FU-treated (■) or nontreated (●) MC38 cells. (*b*) In some experiments, the cytolytic ability of activated NK cells was assessed by a 4-hr ^{51}Cr-release assay with or without blocking Abs against Rae-1 or H60 at an E/T ratio of 30:1. Similar results were obtained from 3 independent experiments. $*p < 0.05$ *versus* the cytolytic activity of activated NK cells against nontreated cells, $\#p < 0.05$ *versus* the cytolytic activity of activated NK cells against 5-FU-treated cells.

5-FU is not toxic to hepatocytes and does not harm the liver or kidney.

α-GalCer, but not 5-FU, treatment induced NK activating receptors on NK cells

We examined the expression levels of activating (NKG2D and DNAM1) receptors on liver NK cells. C57BL/6 mice were treated with α-GalCer (0.4 μg/mouse) i.p. on Day 0 or 5-FU (10 mg/kg body weight) for 3 consecutive days and liver NK cells were isolated from 5-FU- and α-GalCer-treated mice. As shown in Figure 2, the expression levels of NKG2D and DNAM1 on liver NK cells from α-GalCer-treated mice were significantly higher than those from PBS-treated mice. In contrast, the expression of NKG2D and DNAM1 on liver NK cells from 5-FU-treated mice was similar to that of PBS-treated mice. These results demonstrated that α-GalCer, but not 5-FU, could activate liver NK cells.

5-FU, but not α-GalCer, treatment induced NK activating molecules on colon cancer cells

We next examined the expression of the NKG2D ligands (Rae-1 and H60) and DNAM1 ligands (CD112 and CD155) on MC38 colon cancer cells treated with α-GalCer and/or 5-FU. We first examined the cytotoxicity of 5-FU on MC38 cells by the WST-8 assay. The addition of more than 1 μmol/l of 5-FU resulted in a significant decrease in the growth of MC38 cells (data not shown). On the basis of these findings, we used 500 nmol/l of 5-FU to evaluate the biological effect on MC38 cells. MC38 cells were incubated with α-GalCer (100 ng/ml) and/or 5-FU (500 nmol/l) for 24 hr and the expression levels of NK activating molecules on MC38 cells were evaluated by flow cytometry. 5-FU induced the expression of Rae-1, H60, CD112, and CD155 on MC38 cells (Fig. 3). The expression of these molecules on 5-FU-treated MC 38 cells was significantly higher than that of nontreated MC38 cells. The induction of these NK activating molecules was dose-dependent (data not shown). In contrast, α-GalCer could not induce the expression of Rae-1, H60, CD112, or CD155 on MC38 cells. Even in the MC38 cells treated with this combination of α-GalCer and 5-FU, α-GalCer failed to induce additional expression of NK activating molecules. These results demonstrated that 5-FU, but not α-GalCer, could enhance the expression of NK activating molecules on colon cancer cells.

The cytolytic activity of α-GalCer activated liver MNCs against 5-FU-treated MC38 cells

We next examined the cytolytic activity of α-GalCer-activated liver MNCs against 5-FU-treated MC38 cells. We isolated liver MNCs from normal α-GalCer injected mice and the cytolytic activity of these α-GalCer-activated liver MNCs was measured. The cytolytic activity of liver MNCs against 5-FU-treated MC38 cells was significantly higher than that against nontreated cells (Fig. 4*a*). The cytolytic activity against 5-FU-treated MC38 cells decreased significantly following the addition of blocking Abs against Rae-1 or H60 (Fig. 4*b*).

5-FU treatment induced the expression of NK activating molecules in MC38 liver tumor tissues but not in MC38 nontumor tissues

We examined the induction of NKG2D ligand (Rae-1 and H60) and DNAM1 ligand (CD112 and CD155) expression in MC38 liver tumor or nontumor tissues of 5-FU-treated mice. As shown in Figure 5, the expression of Rae-1 in liver tumor tissues of 5-FU-treated mice was significantly higher than that of liver tumor and nontumor tissues of PBS-treated mice and that of nontumor tissues of 5-FU-treated mice. The expression of H60 and CD112 was similar to that of Rae-1. The expression of CD155 in liver tumor tissues of 5-FU-treated mice tended to be higher than that of PBS-treated mice, although the difference was not statistically significant. These results demonstrated that 5-FU treatment induced the expression of NK activating molecules in liver tumor tissues but not in nontumor tissues consistent with the *in vitro* results.

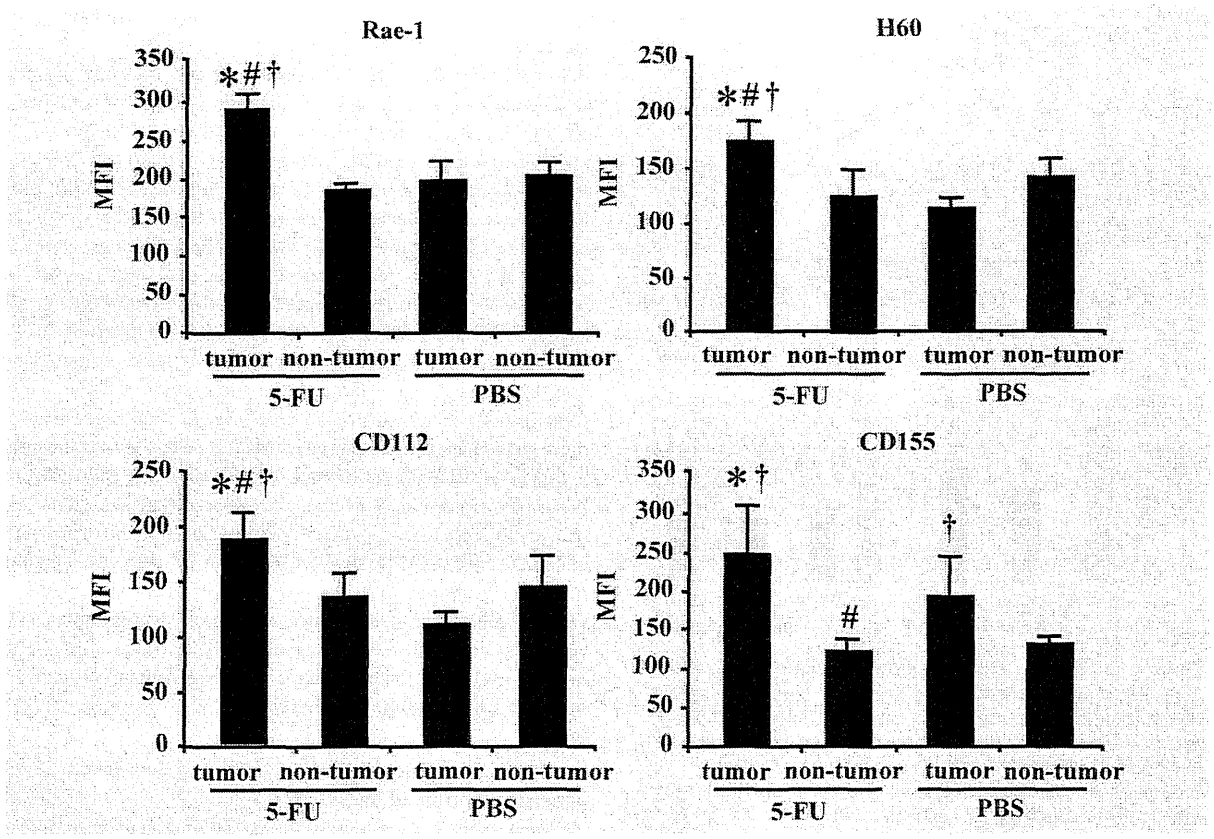

Figure 5. Expression of NKG2D ligands (Rae-1 and H60) and DNAM1 ligands (CD112 and CD155) on MC38 liver tumor tissues of mice treated with 5-FU. C57BL/6 mice were injected in the liver with 3×10^5 MC38 cells on Day 0 and were treated with 5-FU on Day 4–8 after tumor inoculation. On Day 8, MC38 liver tumor or nontumor tissues were harvested and divided into single cells to evaluate the expression of NKG2D ligands (Rae-1 and H60) and DNAM1 ligands (CD112 and CD155) by flow cytometry. $N = 3$/group. *$p < 0.05$ *versus* nontumor tissues of PBS group, #$p < 0.05$ *versus* tumor tissues of PBS group, †$p < 0.05$ *versus* nontumor tissues of 5-FU group.

The antitumor effect of 5-FU depended on both direct cytotoxicity and the cytolytic activity of NK cells in mouse colon cancer

The above results suggested that 5-FU could enhance the NK sensitivity of MC38 cells. To confirm that NK activity played a role in the antitumor effect of 5-FU, we examined the antitumor effect of 5-FU against MC38 liver tumors in NK depleted mice. As shown in Figure 6, the liver weights of 5-FU-treated mice were significantly lower than those of vehicle-treated mice. Depletion of NK cells significantly inhibited the antitumor efficacy of 5-FU against MC38 liver tumors. These results suggested that the antitumor effect of 5-FU depended on not only on the direct cytotoxic effect of 5-FU but also on the cytolytic activity of NK cells. Therefore, NK activity plays a role in the antitumor effect of 5-FU in the liver which contains abundant NK cells.

Discussion

The lymphocytes in the liver are typically enriched with a higher number of NK cells than that found in the peripheral blood in a normal mouse.[3,4] Efficient activation of the abundant NK cells in the liver might be important in antitumor defense against liver tumors. Interferon-α (IFN-α) could activate liver NK cells efficiently.[14] Bui *et al.*[15] reported that IFN-α reduced the expression of H60 on MCA sarcoma cells, suggesting that IFN-α treatment may reduce the NK sensitivity of cancer cells. We and others have previously demonstrated that the systemic administration of α-GalCer can lead to antitumor effects against metastatic liver tumors through the efficient activation of liver NK cells.[8,16] Although α-GalCer has not yet been officially accepted for clinical application in cancer treatment, these previous results encouraged us to evaluate the antitumor effect of the combination of α-GalCer and 5-FU against MC38 liver tumors. In most reports, high dose (2 μg/mouse) α-GalCer was applied for the treatment of liver tumors. However, administration of these high dose resulted in liver injury.[9,17,18] In the present study, we used low dose (0.4 μg/mouse) α-GalCer in the combination therapy. The administration of low dose α-GalCer is enough to activate liver NK cells and did not affect